PTEP

Prog. Theor. Exp. Phys. **2022** 093B11(29 pages)
DOI: 10.1093/ptep/ptac116

IYBSSD2022
International Year
of Basic Sciences
for Sustainable Development

Lepton masses and mixings, and muon anomalous magnetic moment in an extended $B - L$ model with the type-I seesaw mechanism

V. V. Vien[1,2], Hoang Ngoc Long[3], and A. E. Cárcamo Hernández[4,5,6]

[1] *Institute of Applied Technology, Thu Dau Mot University, Binh Duong Province, Vietnam*
[2] *Department of Physics, Tay Nguyen University, DakLak Province, Vietnam*
[3] *Institute of Physics, Vietnam Academy of Science and Technology, 10 Dao Tan, Ba Dinh, 10000 Hanoi, Vietnam*
[4] *Universidad Técnica Federico Santa María, Casilla 110-V, Valparaíso, Chile*
[5] *Centro Científico-Tecnológico de Valparaíso, Casilla 110-V, Valparaíso, Chile*
[6] *Millennium Institute for Subatomic Physics at the High-Energy Frontier - SAPHIR, Fernandez Concha 700, Santiago, Chile*

*E-mail: vovanvien@tdmu.edu.vn

Received June 15, 2022; Revised July 25, 2022; Accepted September 14, 2022; Published September 16, 2022

We propose a $B - L$ model combined with the $S_4 \times Z_3 \times Z_4$ discrete symmetry that successfully explains the recent 3+1 sterile–active neutrino data. The smallness of the neutrino mass is obtained through the type-I seesaw mechanism. The active–active and sterile–active neutrino mixing angles are predicted to be consistent with the recent constraints in which $0.3401\,(0.3402) \leq \sin^2\theta_{12} \leq 0.3415\,(0.3416)$, $0.456\,(0.433) \leq \sin^2\theta_{23} \leq 0.544\,(0.545)$, $2.00\,(2.018) \leq 10^2 \times \sin^2\theta_{13} \leq 2.405\,(2.424)$, $156\,(140.8) \leq \delta_{CP}^{(\circ)} \leq 172\,(167.2)$ for normal (inverted) ordering of the three-neutrino scenario, and $0.015\,(0.022) \leq s_{14}^2 \leq 0.045\,(0.029)$, $0.005(0.0095) \leq s_{24}^2 \leq 0.012\,(0.012)$, $0.003\,(0.009) \leq s_{34}^2 \leq 0.011$ for normal (inverted) ordering of the 3+1 neutrino scenario. Our model predicts flavor-conserving leptonic neutral scalar interactions and successfully explains the muon $g - 2$ anomaly.

Subject Index B40, B54

1. Introduction

Recently, there have been experimental observations that cannot be explained by the three-neutrino oscillation framework [1–13]. However, these observations could be explained by adding at least one additional neutrino (called a sterile neutrino) with mass in the eV range having non-trivial mixing with active neutrinos. The mentioned sterile neutrinos are singlets under $SU(2)_L$ and do not take part in the weak interaction but mix with the active ones that can be verified in the oscillation experiments. Nowadays, there are a number of schemes favoring the existence of sterile neutrinos, including: the (3+1) scheme [13–29] in which one sterile neutrino with mass on the eV scale is heavier than the three active ones, the (3+1+1) scheme

Funded by SCOAP[3]. SCOAP3 and OUP support the goals of the International Year of Basic Sciences for Sustainable Development

Table 1. The neutrino oscillation data for the three-neutrino scheme at 3σ range with the best-fit points taken from Ref. [45] and 3+1 neutrino mixing constraints taken from Ref. [46].

Parameters	3σ range (best fit)	
	Normal hierarchy (NH)	Inverted hierarchy (IH)
$\Delta m^2_{21}(10^{-5}\,\text{eV}^2)$	$6.94 \to 8.14\,(7.50)$	$6.94 \to 8.14\,(7.50)$
$\lvert\Delta m^2_{31}\rvert(10^{-3}\,\text{eV}^2)$	$2.47 \to 2.63\,(2.55)$	$2.37 \to 2.53\,(2.45)$
$s^2_{12}/10^{-1}$	$2.71 \to 3.69\,(3.18)$	$2.71 \to 3.69\,(3.18)$
$s^2_{23}/10^{-1}$	$4.34 \to 6.10\,(5.74)$	$4.33 \to 6.08\,(5.78)$
$s^2_{13}/10^{-2}$	$2.000 \to 2.405\,(2.200)$	$2.018 \to 2.424\,(2.225)$
δ/π	$0.71 \to 1.99\,(1.08)$	$1.11 \to 1.96\,(1.58)$
s^2_{14}	$0.0098 \to 0.0310$	$0.0098 \to 0.0310$
s^2_{24}	$0.0059 \to 0.0262$	$0.0059 \to 0.0262$
s^2_{34}	$0 \to 0.0369$	$0 \to 0.0369$

[30–34] with one sterile neutrino with mass on the eV scale and the other much heavier than 1 eV; the (1+3+1) scheme [35–37] in which one of the sterile neutrinos is lighter than the three active ones and the other is heavier, and the (3+2) scheme [38–44] in which two sterile neutrinos lighter than the three active ones are added to the standard three-neutrino oscillation framework. Among the schemes with sterile neutrinos, the one with one additional sterile neutrino with mass in the eV range (called the four-neutrino scheme) is the simplest extension of standard three-neutrino mixing that can accommodate the anomalous results of short-baseline neutrino oscillations. Among the four-neutrino schemes, the 3+1 scheme is preferred because the 1+3 scheme, whose one sterile neutrino is lighter than the active ones and in which the three active neutrinos are on the eV scale, is ruled out by cosmology while the 2+2 scheme is not suitable with the atmospheric and the solar neutrino oscillation data. The neutrino mass-squared differences and the mixing angles in the three-neutrino scheme [45] and 3+1 neutrino mixing angles [46], at the best-fit points and in the 3σ range, are shown in Table 1. In addition, the 3σ CL ranges of the magnitudes of the elements of the leptonic mixing matrix for the three-neutrino scheme are [47]:

$$\left|U^{3\sigma}_{\text{with SK-atm}}\right| = \begin{pmatrix} 0.801 \to 0.845 & 0.513 \to 0.579 & 0.143 \to 0.155 \\ 0.234 \to 0.500 & 0.417 \to 0.689 & 0.637 \to 0.776 \\ 0.271 \to 0.535 & 0.477 \to 0.694 & 0.613 \to 0.756 \end{pmatrix}. \tag{1}$$

One notable attribute of discrete symmetries is that they provide an explanation for the neutrino oscillation data. For the 3+1 scheme, the $U(1)_{B-L}$ extension with S_3 symmetry was presented in Ref. [48] without mentioning the sterile–active neutrino mass and mixing, which has been addressed in Ref. [49] with results achieved at the first-order approximation, and only the normal mass spectrum was mentioned. The sterile neutrino issue has also been considered in Refs. [50–57] with A_4 symmetry and a very large number of scalar fields, which is substantially different than the model considered in this paper whose scalar sector has a moderate amount of particle content. Namely, in Refs. [50,51] the Standard Model (SM) symmetry is enlarged by the inclusion of the $A_4 \times Z_3 \times U(1)_R$ discrete group. In Ref. [52], the SM symmetry is enlarged by the $A_4 \times Z_4$ symmetry in which only $|U_{e4}|$ has been predicted without $|U_{\mu 4}|$ and $|U_{\tau 4}|$; in Ref. [53], the SM symmetry is enlarged by the symmetry $A_4 \times Z_3 \times Z_3^{'} \times U(1)_R$ where two doublets and 17 singlets are used; in Ref. [54], the symmetry $A_4 \times Z_3 \times Z_4$ is added to the SM in which

Table 2. The particle and scalar contents of the model.

Fields	ψ_L	$l_{1R}(l_{\alpha R})$	$H\,(H')$	$\phi\,(\varphi)$	ρ	χ	ϕ_s	ν_R	ν_s
$[\mathrm{SU}(2)_L, \mathrm{U}(1)_Y]$	$[\mathbf{2}, -1/2]$	$[\mathbf{1}, -1]$	$[\mathbf{2}, 1/2]$	$[\mathbf{1}, 0]$	$[\mathbf{1}, 0]$	$[\mathbf{1}, 0]$	$[\mathbf{1}, 0]$	$[\mathbf{1}, 0]$	$[\mathbf{1}, 0]$
$\mathrm{U}(1)_{B-L}$	-1	-1	0	0	0	2	0	-1	-1
S_4	**3**	**1(2)**	**1 (1′)**	**3**	**1**	**1**	**3**	**3**	**1**
Z_3	ω	1	1	$\omega\,(1)$	1	ω	ω^2	ω	ω^2
Z_4	i	1	1	i	i	1	i	1	$-i$

up to three Higgs doublets and 12 singlets are considered in the scalar sector; in Ref. [55] the symmetry $A_4 \times Z_4$ is added to the SM in which one doublet and up to 12 singlet scalars are introduced; in Ref. [56], the symmetry $A_4 \times C_4 \times C_6 \times C_2 \times U(1)_s$ is added to the SM in which one doublet and up to 12 singlets are used, and only the normal mass spectrum is satisfied; and in Ref. [57], the symmetry $A_4 \times Z_3 \times Z_4$ is added to the $B - L$ in which one Higgs doublet and up to 11 singlets are considered in the scalar sector and without mention of the muon anomalous magnetic moment. Thus, it would be useful to build a S_4 flavored model with a much more economical scalar content. To our knowledge, A_4 has not been considered before in the 3+1 scheme with $B - L$ extension.

This paper is organized as follows. A description of the model is given in Sect. 2. Its implications for lepton masses and mixings as well as the corresponding numerical analysis is presented in Sect. 3. Section 4 is devoted to the muon anomalous magnetic moment. Finally, some conclusions are given in Sect. 5. Appendix B provides the scalar potential of the model.

2. The model

The $B - L$ gauge model [58,59] is supplemented by one discrete symmetry S_4 along with two Abelian symmetries Z_3 and Z_4. Further, three right-handed neutrinos ν_R, one sterile neutrino ν_s, one $SU(2)_L$ doublet ($H^{'}$), and four singlet scalars (ϕ, φ, ρ, ϕ_s) are introduced to the $B - L$ model. Three right-handed neutrinos and three left-handed leptons ψ_L are grouped in **3** under the S_4 symmetry whereas the first right-handed charged lepton l_{1R} is assigned as **1** and the two others are grouped in **2** under the S_4 symmetry. The sterile neutrino ν_s is assigned as **1** under the S_4 symmetry. The particle content of the model under consideration[1] and its corresponding assignments under the symmetry $SU(2)_L \times U(1)_Y \times U(1)_{B-L} \times S_4 \times Z_3 \times Z_4 \equiv \mathbf{\Gamma}$ are shown in Table 2.

With the above-specified particle content, the following 5D Yukawa interactions invariant under the symmetries of the model arise:

$$\begin{aligned}-\mathcal{L}_{clep} = &\frac{x_1}{\Lambda}(\bar{\psi}_L l_{1R})_{\mathbf{3}}(H\phi)_{\mathbf{3}} + \frac{x_2}{\Lambda}(\bar{\psi}_L l_{\alpha R})_{\mathbf{3}}(H\phi)_{\mathbf{3}} + \frac{x_3}{\Lambda}(\bar{\psi}_L l_{\alpha R})_{\mathbf{3}'}(H'\phi)_{\mathbf{3}'} \\ &+ \frac{x_{1\nu}}{\Lambda}(\bar{\psi}_L \nu_R)_{\mathbf{1}}(\widetilde{H}\rho)_{\mathbf{1}} + \frac{x_{2\nu}}{\Lambda}(\bar{\psi}_L \nu_R)_{\mathbf{3}}(\widetilde{H}\varphi)_{\mathbf{3}} + \frac{x_{3\nu}}{\Lambda}(\bar{\psi}_L \nu_R)_{\mathbf{3}'}(\widetilde{H'}\varphi)_{\mathbf{3}'} \\ &+ \frac{y_\nu}{2}(\bar{\nu}_R^c \nu_R)_{\mathbf{1}}\chi + \frac{y_s}{\Lambda}(\bar{\nu}_s^c \nu_R)_{\mathbf{3}}(\chi\phi_s)_{\mathbf{3}} + \mathrm{H.c.}\end{aligned} \tag{2}$$

In Eq. (2), Λ is the cutoff scale of the theory and y_ν, y_s, x_k, and $x_{k\nu}$ ($k = 1, 2, 3$) are dimensionless constants. The VEVs of scalar fields satisfying the scalar potential minimum condition,

[1] Under $SU(3)_C$ symmetry, all leptons and scalars are singlets.

presented in Appendix B, are given as follows:

$$\langle H\rangle = (0 \quad v)^T, \langle H'\rangle = \begin{pmatrix}0 & v'\end{pmatrix}^T, \langle\phi\rangle = (\langle\phi_1\rangle, \ \langle\phi_2\rangle, \ \langle\phi_3\rangle), \ \langle\phi_1\rangle = \langle\phi_2\rangle = \langle\phi_3\rangle = v_\phi,$$

$$\langle\varphi\rangle = (0\langle\varphi_2\rangle 0), \ \langle\varphi_2\rangle = v_\varphi, \ \langle\rho\rangle = v_\rho, \ \langle\chi\rangle = v_\chi, \ \langle\phi_s\rangle = (\langle\phi_{1s}\rangle 0 \langle\phi_{3s}\rangle), \ \langle\phi_{1s}\rangle = \langle\phi_{3s}\rangle = v_s. \quad (3)$$

In fact the electroweak symmetry breaking scale is one order of magnitude lower than the TeV scale and the $B-L$ scale is assumed to be at the TeV scale, i.e.,

$$v' \sim v = 1.23 \times 10^2 \,\text{GeV}, \ v_\chi = 10^3 \,\text{GeV}. \quad (4)$$

Furthermore, in order to have very heavy right-handed Majorana neutrino masses, thus allowing the implementation of the type-I seesaw mechanism that produces the tiny masses of the active neutrinos, the VEVs of flavons ϕ, φ, ρ, and ϕ_s are assumed to be at a very high scale:

$$v_\phi \sim v_\varphi \sim v_\rho \sim v_{\phi_s} = 10^{11} \,\text{GeV}. \quad (5)$$

It is interesting to note that each additional symmetry $U(1)_{B-L}$, S_4, Z_3, and Z_4 plays a crucial role in forbidding the unwanted terms, which are listed in Table A1 of Appendix A, to obtain the lepton mass matrices in Eqs. (7) and (19). Furthermore, there exist invariant terms via Weinberg operators with dimensions greater than or equal to six, $\frac{1}{\Lambda^{2(k+l+1)}}(\overline{\psi}_L\psi_L^c)(\widetilde{\mathbf{H}}^2\chi^*)(\mathbf{H}^\dagger\mathbf{H})^k(\mathbf{P}^*\mathbf{P})^l$ with $k, l = 0, 1, 2, \ldots$; $\mathbf{H} = H, H'$ and $\mathbf{P} = \phi, \varphi, \rho, \chi, \phi_s$. The fact that $v_H \ll v_\mathbf{P} \ll \Lambda$ means that the neutrino mass obtained by those Weinberg operators, $v_\mathbf{H}\left(\frac{v_\mathbf{H}}{\Lambda}\right)^{2k+1}\left(\frac{v_P}{\Lambda}\right)^{2l+1}$, is very small compared to the one obtained by the type-I seesaw mechanism as in Eq. (19) and thus has been ignored.

3. Neutrino mass and mixing

3.1 *Lepton mass and mixing in the three-neutrino framework*

From the Yukawa interactions in Eq. (2), and using the tensor product rules of the S_4 discrete group [60], together with the VEVs of scalar fields in Eq. (3), the charged lepton mass Lagrangian is written in the form:

$$\mathcal{L}_{cl}^{\text{mass}} = -(\bar{l}_{1L}\,\bar{l}_{2L}\,\bar{l}_{3L})M_l(l_{1R}\,l_{2R}\,l_{3R})^T + \text{H.c.}, \quad (6)$$

where

$$M_l = \begin{pmatrix} x_1 v\frac{v_\phi}{\Lambda} & \frac{v_\phi}{\Lambda}(x_2 v + x_3 v') & \frac{v_\phi}{\Lambda}(x_2 v - x_3 v') \\ x_1 v\frac{v_\phi}{\Lambda} & \omega^2\frac{v_\phi}{\Lambda}(x_2 v + x_3 v') & \omega\frac{v_\phi}{\Lambda}(x_2 v - x_3 v') \\ x_1 v\frac{v_\phi}{\Lambda} & \omega\frac{v_\phi}{\Lambda}(x_2 v + x_3 v') & \omega^2\frac{v_\phi}{\Lambda}(x_2 v - x_3 v') \end{pmatrix}, \quad (7)$$

which is diagonalized as, $U_l^\dagger M_l U_r = \text{diag}(m_e, \ m_\mu, \ m_\tau)$, with

$$U_l^\dagger = \frac{1}{\sqrt{3}}\begin{pmatrix} 1 & 1 & 1 \\ 1 & \omega & \omega^2 \\ 1 & \omega^2 & \omega \end{pmatrix}, \ U_r = \mathbf{I}_{3\times 3} \quad \left(\omega = e^{\frac{i2\pi}{3}}\right), \quad (8)$$

$$m_e = \sqrt{3}x_1 v\frac{v_\phi}{\Lambda}, \ m_{\mu,\tau} = \sqrt{3}\frac{v_\phi}{\Lambda}\left(x_2 v \pm x_3 v'\right). \quad (9)$$

Equation (8) tells us that U_l is non-trivial and hence it will affect the lepton mixing matrix. Furthermore, Eq. (9) shows that m_μ and m_τ are distinguished by v'. This is the reason why H' is additionally introduced to H.

Furthermore, assuming that the gauge singlet scalar fields require VEVs much larger than the electroweak symmetry breaking scale, the scalar spectrum at low energies is the same as in the 2HDM theory. Then, the physical CP-even and CP-odd neutral scalar fields are given by:

$$H_R^0 = \sin\alpha h - \cos\alpha H, \qquad H_R'^0 = -\cos\alpha h - \sin\alpha H, \quad (10)$$

$$H_I^0 = \cos\beta G_Z + \sin\beta A^0, \quad H_I'^0 = \sin\beta G_Z - \cos\beta A^0, \tag{11}$$

where G_Z is the Goldstone boson associated with the longitudinal component of the gauge boson Z, h is the 126 GeV SM-like Higgs, H is the heavy CP-even Higgs, A is the heavy CP-odd Higgs boson, $\tan\beta = \frac{v}{v'}$, and α is the mixing angle in the neutral scalar sector. Then, the leptonic Yukawa interactions involving neutral scalar fields are given by:

$$\begin{aligned}\mathcal{L}_Y^h &= \sqrt{\frac{3}{2}} y_1 \sin\alpha \bar{e}_L h e_R + \sqrt{\frac{3}{2}} \left(y_2 \sin\alpha - y_3 \cos\alpha\right) \overline{\mu}_L h \mu_R \\ &\quad + \sqrt{\frac{3}{2}} \left(y_2 \sin\alpha + y_3 \cos\alpha\right) \overline{\tau}_L h \tau_R + \text{H.c.}, \end{aligned} \tag{12}$$

$$\begin{aligned}\mathcal{L}_Y^{H^0} &= -\sqrt{\frac{3}{2}} y_1 \cos\alpha \bar{e}_L H^0 e_R + \sqrt{\frac{3}{2}} \left(y_2 \cos\alpha + y_3 \sin\alpha\right) \overline{\mu}_L H^0 \mu_R \\ &\quad + \sqrt{\frac{3}{2}} \left(y_2 \cos\alpha - y_3 \sin\alpha\right) \overline{\tau}_L H^0 \tau_R + \text{H.c.}, \end{aligned} \tag{13}$$

$$\begin{aligned}\mathcal{L}_Y^{A^0} &= i\sqrt{\frac{3}{2}} y_1 \sin\beta \bar{e}_L A^0 e_R + i\sqrt{\frac{3}{2}} \left(y_2 \sin\beta - y_3 \cos\beta\right) \overline{\mu}_L A^0 \mu_R \\ &\quad + i\sqrt{\frac{3}{2}} \left(y_2 \sin\beta + y_3 \cos\beta\right) \overline{\tau}_L A^0 \tau_R + \text{H.c.}, \end{aligned} \tag{14}$$

where

$$y_k = x_k \frac{v_\phi}{\Lambda} \quad (k = 1, 2, 3). \tag{15}$$

Equations (12), (13), and (14) imply that the flavor-changing leptonic neutral scalar interactions are absent in our model. Consequently, there are no scalar contributions to the charged lepton flavor-violating decays $\tau \to \mu\gamma$, $\tau \to e\gamma$, and $\mu \to e\gamma$. The charged lepton flavor-violating decays $\tau \to \mu\gamma$, $\tau \to e\gamma$, and $\mu \to e\gamma$ will receive one-loop level contributions due to the electrically charged scalars and right-handed Majorana neutrinos; however, these contributions will scale with the inverse of the fourth power of the model cutoff as well as with the fourth power of the very small neutrino Yukawa coupling, thus making their branching ratios very tiny. Other contributions to the charged lepton flavor-violating decays will arise from the virtual exchange of a W gauge boson and sterile neutrinos; however, these contributions will have very tiny branching ratios as in the SM.

As we will see in the following, our model can successfully accommodate the SM charged lepton masses. Now, comparing the obtained result in Eq. (9) with the experimental values of $m_{e,\,\mu,\,\tau}$ [61], $m_e = 0.510\,99\,\text{MeV}$, $m_\mu = 105.658\,37\,\text{MeV}$, $m_\tau = 1776.86\,\text{MeV}$, and considering the benchmark point $v = v' = 123\,\text{GeV}$, $v_\phi = 10^{11}\,\text{GeV}$, and $\Lambda = 10^{13}\,\text{GeV}$, we get:

$$|x_1| \sim 10^{-4}, \; |x_2| \sim |x_3| \sim 10^{-1}. \tag{16}$$

Furthermore, from the leptonic Yukawa interactions and using the benchmark point given above, it follows that the coupling of the 126 GeV SM-like Higgs boson with the SM lepton–antilepton pair is about 0.7 of the SM expectation.

From the particle content given in Table 2, we get the following neutrino Yukawa interactions:

$$\begin{aligned}-\mathcal{L}_Y^l &= \frac{x_{1\nu}}{\Lambda}(\bar{\psi}_{1L}\nu_{1R} + \bar{\psi}_{2L}\nu_{2R} + \bar{\psi}_{3L}\nu_{3R})\widetilde{H}\rho \\ &+ \frac{x_{2\nu}}{\Lambda}\left[(\bar{\psi}_{2L}\nu_{3R} + \bar{\psi}_{3L}\nu_{2R})(\widetilde{H}\varphi_1) + (\bar{\psi}_{3L}\nu_{1R} + \bar{\psi}_{1L}\nu_{3R})(\widetilde{H}\varphi_2) + (\bar{\psi}_{1L}\nu_{2R} + \bar{\psi}_{2L}\nu_{1R})(\widetilde{H}\varphi_3)\right] \\ &+ \frac{x_{3\nu}}{\Lambda}\left[(\bar{\psi}_{2L}\nu_{3R} - \bar{\psi}_{3L}\nu_{2R})(\widetilde{H'}\varphi_1) + (\bar{\psi}_{3L}\nu_{1R} - \bar{\psi}_{1L}\nu_{3R})(\widetilde{H'}\varphi_2) + (\bar{\psi}_{1L}\nu_{2R} - \bar{\psi}_{2L}\nu_{1R})(\widetilde{H'}\varphi_3)\right] \\ &+ \frac{y_\nu}{2}(\bar{\nu}_{1R}^c\nu_{1R} + \bar{\nu}_{2R}^c\nu_{2R} + \bar{\nu}_{3R}^c\nu_{3R})\chi + \frac{y_s}{\Lambda}\left(\bar{\nu}_s^c\nu_{1R}\chi\phi_{1s} + \bar{\nu}_s^c\nu_{2R}\chi\phi_{2s} + \bar{\nu}_s^c\nu_{3R}\chi\phi_{3s}\right) + \text{H.c.} \end{aligned} \tag{17}$$

With the VEV configuration given in Eq. (3), after symmetry breaking, the 7×7 neutrino mass matrix in the (ν_L^c, ν_R, ν_s) basis takes the form

$$M_\nu^{7\times 7} = \begin{pmatrix} 0 & M_D & 0 \\ M_D^T & M_R & M_S^T \\ 0 & M_S & 0 \end{pmatrix}, \tag{18}$$

where M_D, M_R, and M_S are the Dirac, Majorana, and sterile neutrino mass matrices, respectively. They are given by:

$$\begin{aligned} M_D &= \begin{pmatrix} \frac{v_\rho}{\Lambda}vx_{1\nu} & 0 & \frac{v_\varphi}{\Lambda}(vx_{2\nu} - v'x_{3\nu}) \\ 0 & \frac{v_\rho}{\Lambda}vx_{1\nu} & 0 \\ \frac{v_\varphi}{\Lambda}(vx_{2\nu} + v'x_{3\nu}) & 0 & \frac{v_\rho}{\Lambda}vx_{1\nu} \end{pmatrix}, \\ M_R &= y_\nu v_\chi \mathbf{I}, \;\; M_S = y_s v_\chi \frac{v_s}{\Lambda}(1 \quad 0 \quad 1). \end{aligned} \tag{19}$$

In the case of $M_D < M_S \ll M_R$, the effective 4×4 light neutrino mass matrix is determined by [50,52,54,56]:

$$M_\nu = -\begin{pmatrix} M_D M_R^{-1} M_D^T & M_D M_R^{-1} M_S^T \\ M_S \left(M_R^{-1}\right)^T M_D^T & M_S M_R^{-1} M_S^T \end{pmatrix}. \tag{20}$$

The expression (19) shows that, in the neutrino sector, there are five complex parameters, thus implying the existence of 10 real parameters. Considering the case of real VEVs for the scalars H, H', ϕ, χ, and η while taking the VEV of φ to be complex ($v_\varphi = v_0 e^{i\alpha}$), the phase redefinition of ψ_L and ν_R allows the phases of three Yukawa couplings $x_{1\nu}$, y_ν, and y_s to rotate away, reducing this to seven parameters. Furthermore, two parameters are absorbed during the formation of the neutrino mass matrix. Thus, five real and dimensionless parameters $k_{2,3}$, m, m_s, and α are left, where $k_{2,3}$, m, and m_s are defined as follows:

$$k_2 = \frac{v_0}{v_\rho}\frac{x_{2\nu}}{x_{1\nu}}, \; k_3 = \frac{v_0}{v_\rho}\frac{v'}{v}\frac{x_{3\nu}}{x_{1\nu}}, \; m = \frac{v^2 v_\rho^2 x_{1\nu}^2}{\Lambda^2 v_\chi y_\nu}, \; m_s = \frac{2v_\chi v_s^2 y_s^2}{\Lambda^2 y_\nu}. \tag{21}$$

Combining Eqs. (19) and (20) yields the 4×4 active–sterile mass matrix in the explicit form

$$M_\nu^{4\times 4} = -\begin{pmatrix} m\begin{pmatrix} 1+(k_2-k_3)^2e^{2i\alpha} & 0 & 2k_2e^{i\alpha} \\ 0 & 1 & 0 \\ 2k_2e^{i\alpha} & 0 & 1+(k_2+k_3)^2e^{2i\alpha} \end{pmatrix} & \sqrt{\frac{mm_s}{2}}\begin{pmatrix} 1+(k_2-k_3)e^{i\alpha} \\ 0 \\ 1+(k_2+k_3)e^{i\alpha} \end{pmatrix} \\ \sqrt{\frac{mm_s}{2}}\begin{pmatrix} 1+(k_2-k_3)e^{i\alpha} & 0 & 1+(k_2+k_3)e^{i\alpha} \end{pmatrix} & m_s \end{pmatrix}. \tag{22}$$

In the case of $M_D < M_S$, one can apply the type-I seesaw mechanism to Eq. (20) to get the active neutrino mass matrix as [50,52,54,56]

$$\begin{aligned} M_\nu &= M_D M_R^{-1} M_S^T (M_S M_R^{-1} M_S^T)^{-1} M_S M_R^{-1} M_D^T - M_D M_R^{-1} M_D^T \\ &= \frac{m}{2}\begin{pmatrix} -\left[(k_2-k_3)e^{i\alpha}-1\right]^2 & 0 & 1+(k_2^2-k_3^2)e^{2i\alpha}-2e^{i\alpha}k_2 \\ 0 & -2 & 0 \\ 1+(k_2^2-k_3^2)e^{2i\alpha}-2e^{i\alpha}k_2 & 0 & -\left[(k_2+k_3)e^{i\alpha}-1\right]^2 \end{pmatrix}. \end{aligned} \tag{23}$$

We note that M_ν is complex because m, $k_{2,3}$, and α are real parameters. Hence, to determine the active neutrino masses, we define a Hermitian matrix $\mathbf{m}_\nu^2$ given by

$$\mathbf{m}_\nu^2 = M_\nu M_\nu^\dagger = \frac{m^2 k_0}{2}\begin{pmatrix} k_- & 0 & 2k_3^2 - k_0 - i2k_3\sin\alpha \\ 0 & \frac{2}{k_0} & 0 \\ 2k_3^2 - k_0 + i2k_3\sin\alpha & 0 & k_+ \end{pmatrix}, \tag{24}$$

where

$$k_0 = 1 + k_2^2 + k_3^2 - 2k_2\cos\alpha,\ k_\mp = 1 + (k_2 \mp k_3)^2 - 2(k_2 \mp k_3)\cos\alpha. \tag{25}$$

The squared matrix $\mathbf{m}_\nu^2$ in Eq. (24) is diagonalized by the rotation matrix U_ν satisfying

$$U_\nu^\dagger \mathbf{m}_\nu^2 U_\nu = \begin{cases} \begin{pmatrix} 0 & 0 & 0 \\ 0 & m^2 & 0 \\ 0 & 0 & m^2 k_0^2 \end{pmatrix}, U_\nu = \begin{pmatrix} g_0(g_1+ig_2) & 0 & -r_0(g_1+ig_2) \\ 0 & 1 & 0 \\ \frac{1}{\sqrt{2}g_0} & 0 & \frac{1}{\sqrt{2}r_0} \end{pmatrix} \text{for} \quad \text{NH}, \\ \begin{pmatrix} m^2 k_0^2 & 0 & 0 \\ 0 & m^2 & 0 \\ 0 & 0 & 0 \end{pmatrix}, U_\nu = \begin{pmatrix} -r_0(g_1+ig_2) & 0 & g_0(g_1+ig_2) \\ 0 & 1 & 0 \\ \frac{1}{\sqrt{2}r_0} & 0 & \frac{1}{\sqrt{2}g_0} \end{pmatrix} \text{for} \quad \text{IH}, \end{cases} \tag{26}$$

where

$$g_0 = \sqrt{\frac{k_0}{k_-}},\ r_0 = \sqrt{\frac{k_0}{k_+}},\ g_1 = \frac{1}{\sqrt{2}} - \frac{\sqrt{2}k_3^2}{k_0},\ g_2 = \frac{\sqrt{2}k_3\sin\alpha}{k_0}. \tag{27}$$

The corresponding leptonic mixing matrix is

$$U_{\rm lep} = U_L^\dagger U_\nu = \begin{cases} \frac{1}{\sqrt{3}}\begin{pmatrix} \frac{1}{\sqrt{2}g_0} + g_0(g_1+ig_2) & 1 & \frac{1}{\sqrt{2}r_0} - (g_1+ig_2)r_0 \\ \frac{\omega^2}{\sqrt{2}g_0} + g_0(g_1+ig_2) & \omega & \frac{\omega^2}{\sqrt{2}r_0} - (g_1+ig_2)r_0 \\ \frac{\omega}{\sqrt{2}g_0} + g_0(g_1+ig_2) & \omega^2 & \frac{\omega}{\sqrt{2}r_0} - (g_1+ig_2)r_0 \end{pmatrix} \text{for} \quad \text{NH}, \\ \frac{1}{\sqrt{3}}\begin{pmatrix} \frac{1}{\sqrt{2}r_0} - (g_1+ig_2)r_0 & 1 & \frac{1}{\sqrt{2}g_0} + g_0(g_1+ig_2) \\ \frac{\omega^2}{\sqrt{2}r_0} - (g_1+ig_2)r_0 & \omega & \frac{\omega^2}{\sqrt{2}g_0} + g_0(g_1+ig_2) \\ \frac{\omega}{\sqrt{2}r_0} - (g_1+ig_2)r_0 & \omega^2 & \frac{\omega}{\sqrt{2}g_0} + g_0(g_1+ig_2) \end{pmatrix} \text{for} \quad \text{IH}. \end{cases} \tag{28}$$

The three light neutrino masses are given by

$$\begin{cases} m_1^2 = 0, & m_2^2 = m^2, & m_3^2 = k_0^2 m^2 & \text{for} & \text{NH}, \\ m_1^2 = k_0^2 m^2, & m_2^2 = m^2, & m_3^2 = 0 & \text{for} & \text{IH}, \end{cases} \tag{29}$$

which implies the neutrino mass ordering should be either $(0, m, mk_0)$ or $(mk_0, m, 0)$. It is important to note that in the considered model both NH ($m_1 < m_2 < m_3$) and IH ($m_3 < m_1 < m_2$) are satisfied due to the fact that k_0 in Eq. (25) can be greater or less than the case in which k_2 and k_3 are real parameters. Hence, the model can predict both NH and IH spectra, which is consistent with the recent experimental data [45] and different from that of Ref. [56] in which only the NH is allowed.

In the three-neutrino scheme [61], the lepton mixing angles are determined from Eq. (28):

$$s_{13}^2 = |\mathrm{U}_{e3}|^2 = \begin{cases} \frac{2}{3}\frac{k_3^2}{k_0} & \text{for} \quad \text{NH}, \\ \frac{2}{3} - \frac{2}{3}\frac{k_3^2}{k_0} & \text{for} \quad \text{IH}, \end{cases} \tag{30}$$

$$s_{12}^2 = \frac{|\mathrm{U}_{e2}|^2}{1-|\mathrm{U}_{e3}|^2} = \frac{1}{3c_{13}^2} \text{ for both NH and IH}, \tag{31}$$

$$s_{23}^2 = \frac{\left|\mathrm{U}_{\mu 3}\right|^2}{1-|\mathrm{U}_{e3}|^2} = \begin{cases} \frac{1}{2} + \frac{\sqrt{3}k_3 \sin\alpha}{3k_0 - 2k_3^2} & \text{for} \quad \text{NH}, \\ \frac{1}{2} - \frac{\sqrt{3}k_3 \sin\alpha}{k_0 + 2k_3^2} & \text{for} \quad \text{IH}, \end{cases} \tag{32}$$

where $s_{ij} = \sin\theta_{ij}$, $c_{ij} = \cos\theta_{ij}$, $t_{12} = \frac{s_{12}}{c_{12}}$, and $t_{23} = \frac{s_{23}}{c_{23}}$ with θ_{ij} are neutrino mixing angles.

Furthermore, from Eqs. (29), we can express m and k_0 in terms of two observables Δm_{21}^2 and Δm_{31}^2 as follows:

$$m = \begin{cases} \sqrt{\Delta m_{21}^2} & \text{for} \quad \text{NH}, \\ \sqrt{\Delta m_{21}^2 - \Delta m_{31}^2} & \text{for} \quad \text{IH}, \end{cases} \tag{33}$$

$$k_0 = \begin{cases} \frac{\sqrt{\Delta m_{31}^2}}{m} & \text{for} \quad \text{NH}, \\ \frac{\sqrt{-\Delta m_{31}^2}}{m} & \text{for} \quad \text{IH}. \end{cases} \tag{34}$$

The fact is that the neutrino mass ordering can be normal ($m_1 < m_2 < m_3$) or inverted ($m_3 < m_1 < m_2$) depending on the sign of Δm_{31}^2 [45,62]. We will show that the considered model can provide a satisfactory explanation of neutrino masses and mixing data for both the three-neutrino scheme and the 3+1 scheme, given in Table 1.

3.2 *3+1 sterile–active neutrino mixing*

In the case of $M_D < M_S$, the mass of the fourth mass eigenstate is given by [50,52,54,56]:

$$m_4 = M_S M_R^{-1} M_S^T = m_s. \tag{35}$$

Combining Eqs. (29) and (35) yields:

$$m_s = m_4 = \begin{cases} \sqrt{\Delta m_{41}^2} & \text{for} \quad \text{NH}, \\ \sqrt{m^2 k_0^2 + \Delta m_{41}^2} & \text{for} \quad \text{IH}. \end{cases} \tag{36}$$

The 4×4 neutrino mixing matrix is given by [50,52,54,56]:

$$U = U_L^\dagger U_\nu = \begin{pmatrix} U_L^\dagger (1 - \frac{1}{2} R R^\dagger) U_\nu & U_L^\dagger R \\ -R^\dagger U_\nu & 1 - \frac{1}{2} R^\dagger R \end{pmatrix}, \tag{37}$$

where R is given by [50,52,54,56]

$$R = M_D M_R^{-1} M_S^T \quad (M_S M_R^{-1} M_S^T \quad)^{-1} = \sqrt{\frac{m}{2m_s}} \begin{pmatrix} 1 + (k_2 - k_3) e^{i\alpha} \\ 0 \\ 1 + (k_2 + k_3) e^{i\alpha} \end{pmatrix}. \tag{38}$$

Combining Eqs. (8) and (38), we find that the strength of the active–sterile mixing is given by

$$U_L^\dagger R = \sqrt{\frac{m}{6m_s}} \begin{pmatrix} 2 + 2k_2 e^{i\alpha} \\ \left[\omega^2 (k_2 + k_3) + k_2 - k_3\right] e^{i\alpha} - \omega \\ \left[\omega (k_2 + k_3) + k_2 - k_3\right] e^{i\alpha} - \omega^2 \end{pmatrix} \equiv \begin{pmatrix} U_{e4} \\ U_{\mu 4} \\ U_{\tau 4} \end{pmatrix}, \tag{39}$$

which leads to

$$s_{14}^2 = |U_{e4}|^2 = \frac{2}{3}\frac{m}{m_s}\left(1 + k_2^2 + 2k_2\cos\alpha\right),$$
$$s_{24}^2 = \frac{|U_{\mu 4}|^2}{1 - |U_{e4}|^2} = \frac{1 + k_2^2 + 3k_3^2 + 2k_2\cos\alpha + 2\sqrt{3}k_3\sin\alpha}{\frac{6m_s}{m} - 4\left(1 + k_2^2 + 2k_2\cos\alpha\right)},$$
$$s_{34}^2 = \frac{|U_{\tau 4}|^2}{1 - |U_{e4}|^2 - |U_{\mu 4}|^2} = \frac{1 + k_2^2 + 3k_3^2 + 2k_2\cos\alpha - 2\sqrt{3}k_3\sin\alpha}{\frac{6m_s}{m} - \left(5 + 5k_2^2 + 3k_3^2 + 10k_2\cos\alpha + 2\sqrt{3}k_3\sin\alpha\right)}. \quad (40)$$

3.3 *Effective neutrino mass parameter and Jarlskog invariant*

The Jarlskog invariant, obtained from Eq. (28), has the form [61,63–65]

$$J_{CP} = \mathrm{Im}(U_{12}U_{23}U_{13}^*U_{22}^*) = \begin{cases} \frac{k_3(k_2-\cos\alpha)}{3\sqrt{3}k_0} & \text{for} \quad \text{NH}, \\ -\frac{k_3(k_2-\cos\alpha)}{3\sqrt{3}k_0} & \text{for} \quad \text{IH}. \end{cases} \quad (41)$$

The effective neutrino masses get the following forms [66–68]:

$$m_\beta^{(3)} = \sqrt{\sum_{i=1}^{3}|U_{ei}|^2 m_i^2} = \sqrt{\frac{m^2}{3} + \frac{m^2 k_0\left[\left(2k_3^2 - k_0 + k_+\right)^2 + 4k_3^2\sin^2\alpha\right]}{6k_+}}, \quad (42)$$

$$\left\langle m_{ee}^{(3)}\right\rangle = \left|\sum_{i=1}^{3}U_{ei}^2 m_i\right|$$
$$= \frac{m}{6}\sqrt{\frac{16k_3^2\sin^2\alpha\left(2k_3^2 - k_0 + k_+\right)^2 + \left[\left(k_+ - k_0 + 2k_3^2\right)^2 - 4k_3^2\sin^2\alpha + 2k_+\right]^2}{k_+^2}}, \quad (43)$$

$$m_\beta = \sqrt{\sum_{i=1}^{4}|U_{ei}|^2 m_i^2} = \left\{\frac{m^2}{3} + \frac{m^2 k_0\left[\left(2k_3^2 - k_0 + k_+\right)^2 + 4k_3^2\sin^2\alpha\right]}{6k_+}\right.$$
$$\left. + \frac{2mm_s}{3}\left[(k_2\cos\alpha + 1)^2 + k_2^2\sin^2\alpha\right]\right\}^{\frac{1}{2}}, \quad (44)$$

$$\langle m_{ee}\rangle = \left|\sum_{i=1}^{4}U_{ei}^2 m_i\right| = \frac{m}{3}\left\{16\sin^2\alpha\left[2k_2k_+(k_2\cos\alpha + 1) + k_0k_3 - 2k_3^3 - k_3k_+\right]^2\right.$$
$$+\left[k_0^2 + 6k_+ + 4k_2k_+(k_2\cos\alpha + 2)\cos\alpha - 2k_0\left(2k_3^2 + k_+\right)\right.$$
$$\left.\left. -4\left(k_2^2k_+ + k_3^2\right)\sin^2\alpha + \left(2k_3^2 + k_+\right)^2\right]^2\right\}^{\frac{1}{2}}. \quad (45)$$

3.4 *Numerical analysis*

Firstly, provided that s_{13} is located inside the 3σ experimentally allowed range[2] taken from Ref. [45], i.e., $s_{13}^2 \in (2.000, 2.405)10^{-2}$ for NH and $s_{13}^2 \in (2.018, 2.424)10^{-2}$ for IH, from Eq. (31),

[2]In the present work, numbers are displayed with four significant digits to the right of the decimal point.

we predict the solar mixing angle:

$$s_{12}^2 \in \begin{cases} (0.3401, 0.3415) & \text{for} \quad \text{NH}, \\ (0.3402, 0.3416) & \text{for} \quad \text{IH}, \end{cases} \tag{46}$$

which is consistent with the 2σ experimental range given in Ref. [45].

Furthermore, Eqs. (33) and (34) imply that

$$m \in \begin{cases} (8.331, 9.022)\,\text{meV} & \text{for} \quad \text{NH}, \\ (49.39, 51.10)\,\text{meV} & \text{for} \quad \text{IH}, \end{cases} \quad k_0 \in \begin{cases} (5.51, 6.16) & \text{for} \quad \text{NH}, \\ (0.9833, 0.9866) & \text{for} \quad \text{IH}, \end{cases} \tag{47}$$

$$\begin{cases} m_1 = 0, \quad m_2 \in (8.331, 9.022)\,\text{meV}, \quad m_3 \in (49.70, 51.28)\,\text{meV} & \text{for} \quad \text{NH}, \\ m_1 \in (48.68, 50.30)\,\text{meV}, \quad m_2 \in (49.39, 50.10)\,\text{meV}, \quad m_3 = 0 & \text{for} \quad \text{IH}, \end{cases} \tag{48}$$

$$\sum\nolimits_{i=1}^{3} m_i \in \begin{cases} (58.03, 60.31)\,\text{meV} & \text{for} \quad \text{NH}, \\ (98.07, 101.30)\,\text{meV} & \text{for} \quad \text{IH}, \end{cases} \tag{49}$$

provided that the light neutrino mass-squared differences Δm_{21}^2 and Δm_{31}^2 are varied in the 3σ range of Ref. [45] as shown in Table 1.

To find the allowed ranges of k_2, k_3, m, m_s, and α and the predictive ranges of the experimental parameters $\sin^2\theta_{23}$, $\sin\delta$, $\langle m_{ee}\rangle$, and s_{k4}^2 $(k = 1, 2, 3)$, we utilize the observables Δm_{21}^2, Δm_{31}^2, Δm_{41}^2, $\sin^2\theta_{13}$, and $\sin^2\theta_{23}$ with values given in Table 1[3].

From Eqs. (25), (30)–(32), and (41), we get:

$$k_2 = \begin{cases} -\frac{1}{s_{13}}\sqrt{\frac{t_N k_\Phi}{2} + \Phi_N + s_{13}^2} & \text{for} \quad \text{NH}, \\ \sqrt{1 + \frac{1}{2-3s_{13}^2}\left(\frac{3t_I k_\Phi}{2} + \sqrt{3}\Phi_I\right)} & \text{for} \quad \text{IH}, \end{cases} \tag{50}$$

$$k_3 = \begin{cases} \sqrt{\frac{3t_N}{2}}\, s_{13} & \text{for} \quad \text{NH}, \\ \sqrt{\left(1 - \frac{3}{2}s_{13}^2\right) t_I} & \text{for} \quad \text{IH}, \end{cases} \tag{51}$$

$$\cos\alpha = \begin{cases} \frac{\sqrt{\frac{t_N k_\Phi}{2} + \Phi_N + s_{13}^2}\left(t_N c_{13}^4 \cos^2 2\theta_{23} + \Phi_N - 2s_{13}^2\right)}{\left[t_N(3s_{13}^2 - 2) + 2\right] s_{13}^3} & \text{for} \quad \text{NH}, \\ \frac{\sqrt{2 - 3s_{13}^2 + \frac{3t_I k_\Phi}{2} + \sqrt{3}\Phi_I}\left(3t_I c_{13}^4 \cos^2 2\theta_{23} + \sqrt{3}\Phi_I + 6s_{13}^2 - 4\right)}{\sqrt{2 - 3s_{13}^2}\left(3t_I s_{13}^2 - 2\right)} & \text{for} \quad \text{IH}, \end{cases} \tag{52}$$

$$\sin\delta_{CP} = \begin{cases} -\frac{\sqrt{t_N k_\Phi + 2(\Phi_N + s_{13}^2)}\left(s_{13} + \frac{t_N c_{13}^4 \cos^2 2\theta_{23} + \Phi_N - 2s_{13}^2}{s_{13}\left[t_N(3s_{13}^2 - 2) + 2\right]}\right)}{\sqrt{t_N}\, s_{13}^2 \sin 2\theta_{23}\sqrt{2 - 3s_{13}^2}} & \text{for} \quad \text{NH}, \\ -\frac{s_{13}\sqrt{2 - 3s_{13}^2 + \frac{3t_I k_\Phi}{2} + \sqrt{3}\Phi_I}\left(\frac{3t_I c_{13}^4 \cos^2 2\theta_{23} + \sqrt{3}\Phi_I + 6s_{13}^2 - 4}{(3s_{13}^2 - 2)\left(3t_N s_{13}^2 - 2\right)} + 1\right)}{\sqrt{6}\, s_{13}^2 s_{23} c_{23}\sqrt{(2 - 3s_{13}^2) t_N}} & \text{for} \quad \text{IH}, \end{cases} \tag{53}$$

with

$$\Phi_N = \sqrt{\left(\cos^2 2\theta_{13} - c_{13}^4 \sin^2 2\theta_{23}\right)\left(t_N c_{13}^4 \cos^2 2\theta_{23} - 2s_{13}^2\right) t_N}, \tag{54}$$

$$\Phi_I = \sqrt{\left(\cos^2 2\theta_{13} - c_{13}^4 \sin^2 2\theta_{23}\right)\left(3t_I c_{13}^4 \cos^2 2\theta_{23} + 6s_{13}^2 - 4\right) t_I}, \tag{55}$$

$$k_\Phi = (6 - 5s_{13}^2)s_{13}^2 + 2(c_{13}^4 \sin^2 2\theta_{23} - 1), \tag{56}$$

[3] As will be mentioned below, at present, there are various experimental bounds on Δm_{41}^2. In this work, Δm_{41}^2 is assumed to be in the range of $\Delta m_{41}^2 \in (5.0, 10)\,\text{eV}^2$ for NH and $\Delta m_{41}^2 \in (30.0, 50.0)\,\text{eV}^2$ for IH.

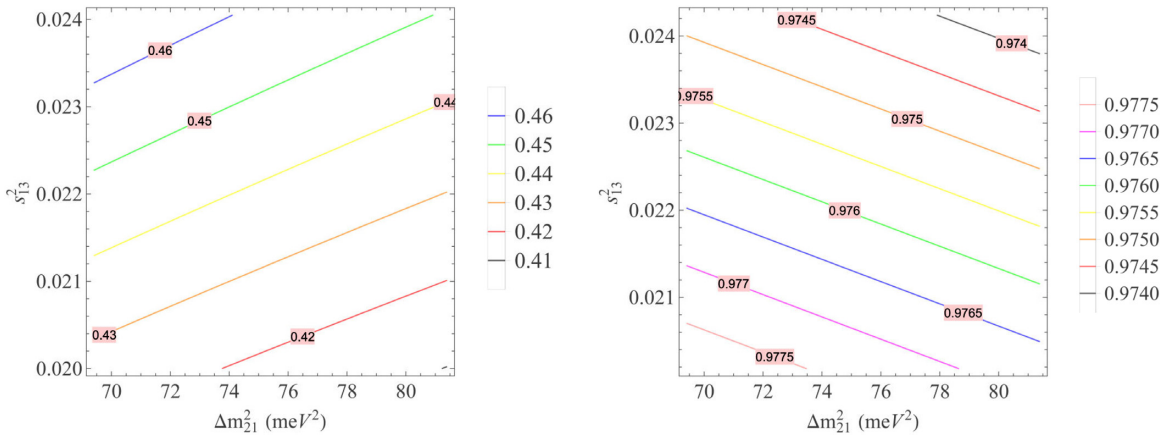

Fig. 1. k_3 as a function of s^2_{13} and Δm^2_{21} with $\Delta m^2_{21} \in (69.4, 81.4)\,\text{meV}^2$ and $s^2_{13} \in (2.000, 2.405)10^{-2}$ for NH (in the left panel) and $s^2_{13} \in (2.018, 2.424)10^{-2}$ for IH (in the right panel).

$$t_N = \sqrt{\frac{\Delta m^2_{31}}{\Delta m^2_{21}}},\ t_I = \sqrt{\frac{-\Delta m^2_{31}}{\Delta m^2_{21} - \Delta m^2_{31}}}. \tag{57}$$

Equations (50)–(57) imply that k_3 depends on three parameters Δm^2_{21}, Δm^2_{31}, and s_{13} while k_2 and $\cos\alpha$ depend on four parameters Δm^2_{21}, Δm^2_{31}, s_{13}, and s_{23}. As a consequence, Eqs. (40)–(57) imply that J_{CP}, $\sin\delta_{CP}$, $\langle m^{(3)}_{ee}\rangle$, $\langle m_{ee}\rangle$, and $m^{(3)}_\beta$ as well as $|U_{ij}|$ $(i = 1, 2, 3;\ j = 1, 3)$ depend on four parameters Δm^2_{21}, Δm^2_{31}, s_{13}, and s_{23} while s^2_{k4} $(k = 1, 2, 3)$ and m_β depend on five parameters Δm^2_{21}, Δm^2_{31}, s_{13}, s_{23}, and $m_s \equiv m_4 \equiv \sqrt{\Delta m^2_{41}}$ in which three parameters Δm^2_{21}, Δm^2_{31}, and s_{13} are measured with more accuracy that can be used to constrain the others.

At the best-fit points of Δm^2_{31} [45], $\Delta m^2_{31} = 2.55 \times 10^3\,\text{meV}^2$ for NH and $\Delta m^2_{31} = -2.45 \times 10^3\,\text{meV}^2$ for IH, the parameter k_3 depends on s^2_{13} and Δm^2_{21}, which is depicted in Fig. 1. This figure implies

$$k_3 \in \begin{cases} (0.41, 0.46) & \text{for NH}, \\ (0.9740, 0.9775) & \text{for IH}. \end{cases} \tag{58}$$

At the best-fit points of two light neutrino mass-squared differences taken from Ref. [45], $\Delta m^2_{31} = 2.55 \times 10^3\,\text{meV}^2$ for NH while $\Delta m^2_{31} = -2.45 \times 10^3\,\text{meV}^2$ for IH and $\Delta m^2_{31} = 75.0\,\text{meV}^2$, we get

$$k_0 = \begin{cases} 5.831 & \text{for NH}, \\ 0.985 & \text{for IH}, \end{cases} \tag{59}$$

and the parameters k_2, $\cos\alpha$, $\sin\delta_{CP}$, $\langle m^{(3)}_{ee}\rangle$, $\langle m_{ee}\rangle$, and $m^{(3)}_\beta$ depend on s_{13} and s_{23}, which are, respectively, depicted below in Figs. 2, 3, 5, 6, 8, and 9.

Figure 2 implies that

$$k_2 \in \begin{cases} (-3.20, -2.40) & \text{for NH}, \\ (1.13, 1.18) & \text{for IH}. \end{cases} \tag{60}$$

From Fig. 3, it follows that:

$$\cos\alpha \in \begin{cases} (-0.90, 0.0) & \text{for NH}, \\ (0.994, 0.999) & \text{for IH}, \end{cases} \text{ i.e., } \alpha^{(\circ)} \in \begin{cases} (90.0, 154.0) & \text{for NH}, \\ (2.563, 6.28) & \text{for IH}. \end{cases} \tag{61}$$

The dependence of J_{CP} on s^2_{23} and s^2_{13} is depicted in Fig. 4.

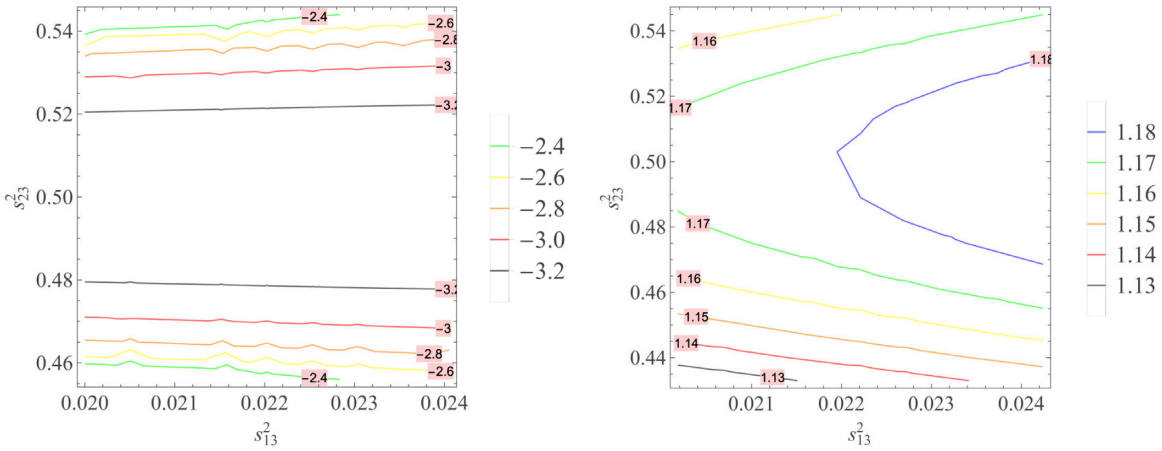

Fig. 2. k_2 as a function of s^2_{23} and s^2_{13} with $s^2_{23} \in (0.456, 0.544)$ and $s^2_{13} \in (2.00, 2.405)10^{-2}$ for NH (in the left panel) and $s^2_{23} \in (0.433, 0.545)$ and $s^2_{13} \in (2.018, 2.424)10^{-2}$ for IH (in the right panel).

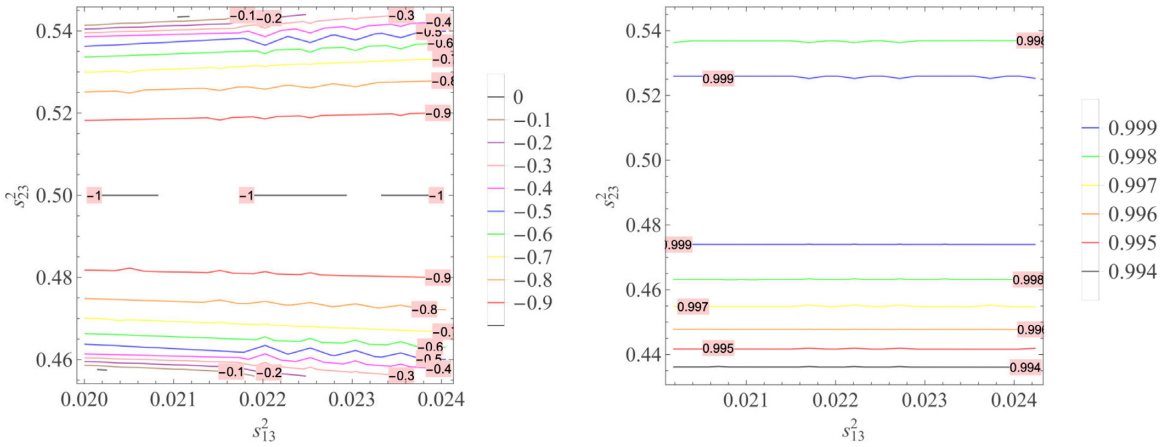

Fig. 3. $\cos\alpha$ as a function of s^2_{23} and s^2_{13} with $s^2_{23} \in (0.456, 0.544)$ and $s^2_{13} \in (2.00, 2.405)10^{-2}$ for NH (in the left panel) and $s^2_{23} \in (0.433, 0.545)$ and $s^2_{13} \in (2.018, 2.424)10^{-2}$ for IH (in the right panel).

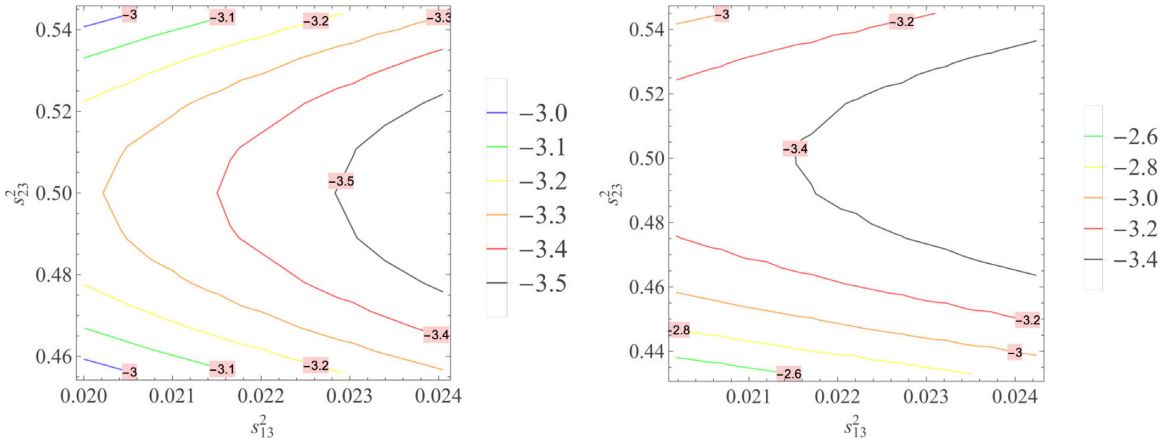

Fig. 4. $J_{CP} \times 10^2$ as a function of s^2_{23} and s^2_{13} with $s^2_{23} \in (0.456, 0.544)$ and $s^2_{13} \in (2.00, 2.405)10^{-2}$ for NH (in the left panel) and $s^2_{23} \in (0.433, 0.545)$ and $s^2_{13} \in (2.018, 2.424)10^{-2}$ for IH (in the right panel).

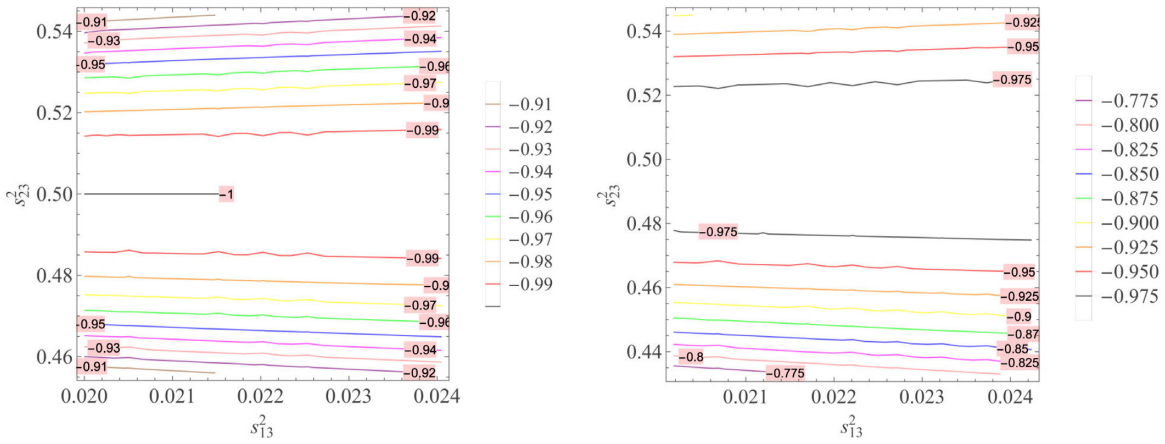

Fig. 5. $\sin\delta_{CP}$ as a function of s^2_{23} and s^2_{13} with $s^2_{23} \in (0.456, 0.545)$ and $s^2_{13} \in (2.00, 2.405)10^{-2}$ for NH (in the left panel) and $s^2_{23} \in (0.433, 0.545)$ and $s^2_{13} \in (2.018, 2.424)10^{-2}$ for IH (in the right panel).

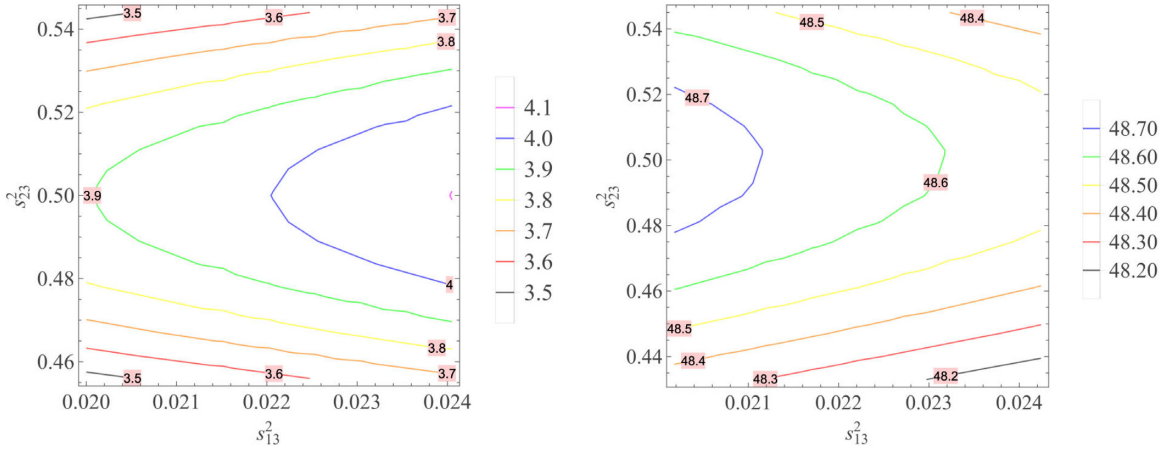

Fig. 6. $\langle m^{(3)}_{ee}\rangle$ (meV) as a function of s^2_{23} and s^2_{13} with $s^2_{23} \in (0.456, 0.544)$ and $s^2_{13} \in (2.00, 2.405)10^{-2}$ for NH (in the left panel) and $s^2_{23} \in (0.433, 0.545)$ and $s^2_{13} \in (2.018, 2.424)10^{-2}$ for IH (in the right panel).

Figure 4 implies that the Jarlskog invariant takes the values [61]:

$$J_{CP} \in \begin{cases} (-3.5, -3.0) \times 10^{-2} & \text{for} \quad \text{NH}, \\ (-3.4, -2.6) \times 10^{-2} & \text{for} \quad \text{IH}. \end{cases} \tag{62}$$

Figure 5 implies that

$$\sin\delta_{CP} \in \begin{cases} (-0.99, -0.91) & \text{for} \quad \text{NH}, \\ (-0.975, -0.775) & \text{for} \quad \text{IH}, \end{cases} \text{ i.e., } \delta^{(\circ)}_{CP} \in \begin{cases} (156.0, 172.0) & \text{for} \quad \text{NH}, \\ (140.8, 167.2) & \text{for} \quad \text{IH}. \end{cases} \tag{63}$$

Figures 6 and 7 imply that

$$\langle m^{(3)}_{ee}\rangle \in \begin{cases} (3.50, 4.10)\,\text{meV} & \text{for} \quad \text{NH}, \\ (48.20, 48.70)\,\text{meV} & \text{for} \quad \text{IH}, \end{cases} \tag{64}$$

$$m^{(3)}_{\beta} \in \begin{cases} (8.80, 9.20)\,\text{meV} & \text{for} \quad \text{NH}, \\ (49.16, 49.24)\,\text{meV} & \text{for} \quad \text{IH}, \end{cases} \tag{65}$$

$$\langle m_{ee}\rangle \in \begin{cases} (40.0, 110.0)\,\text{meV} & \text{for} \quad \text{NH}, \\ (198.0, 208.0)\,\text{meV} & \text{for} \quad \text{IH}. \end{cases} \tag{66}$$

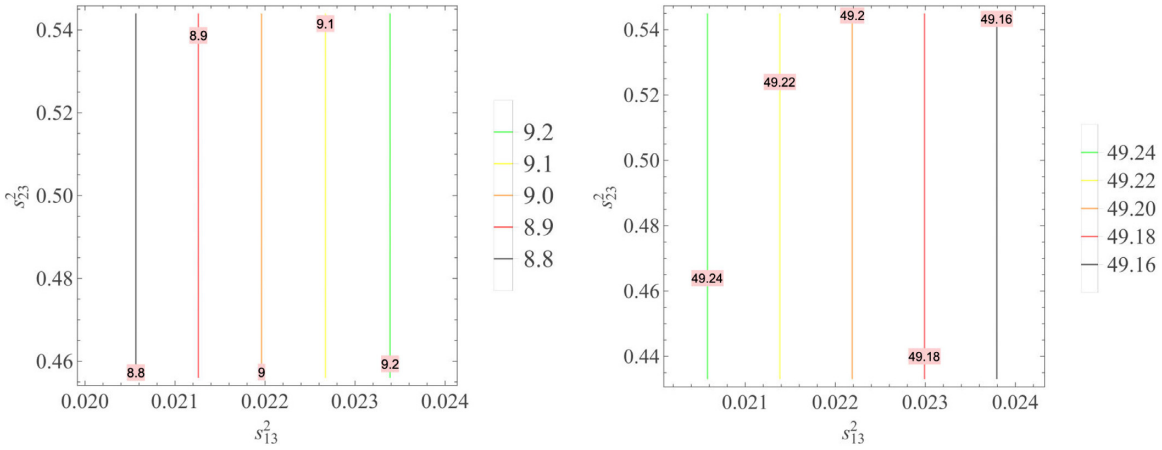

Fig. 7. $m^{(3)}_{\beta}$ (meV) as a function of s^2_{23} and s^2_{13} with $s^2_{23} \in (0.456, 0.544)$ and $s^2_{13} \in (2.00, 2.405)10^{-2}$ for NH (in the left panel) and $s^2_{23} \in (0.433, 0.545)$ and $s^2_{13} \in (2.018, 2.424)10^{-2}$ for IH (in the right panel).

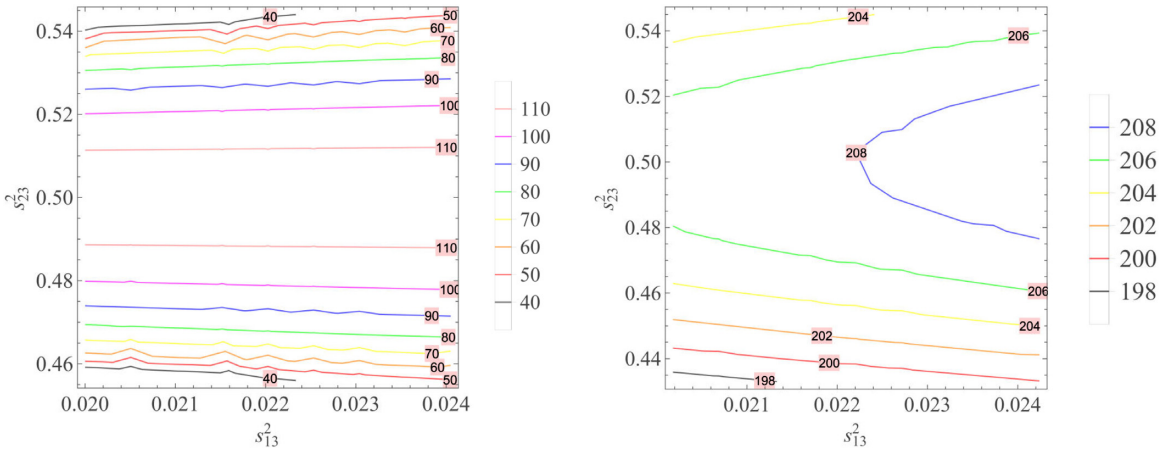

Fig. 8. $\langle m_{ee} \rangle$ (meV) as a function of s^2_{23} and s^2_{13} with $s^2_{23} \in (0.456, 0.544)$ and $s^2_{13} \in (2.00, 2.405)10^{-2}$ for NH (in the left panel) and $s^2_{23} \in (0.541, 0.598)$ and $s^2_{13} \in (2.018, 2.424)10^{-2}$ for IH (in the right panel).

We see that the resulting effective neutrino masses for the three-neutrino scheme in Eqs. (64)–(66), for both NH and IH are below all the upper limits taken from GERDA [69]$\langle m_{ee} \rangle < (120 \div 260)$ meV, MAJORANA [70] $\langle m_{ee} \rangle < (24 \div 53)$ meV, CUORE [71] $\langle m_{ee} \rangle < (110 \div 500)$ meV, KamLAND-Zen [72] $\langle m_{ee} \rangle < (61 \div 165)$ meV, GERDA [73] $\langle m_{ee} \rangle < (104 \div 228)$ meV, CUORE [74] $\langle m_{ee} \rangle < (75 \div 350)$ meV, and CUPID-Mo Collaboration [75] $\langle m_{ee} \rangle < (310 \div 540)$ meV.

The dependence of $\langle m_{ee} \rangle$ on s^2_{23} and Δm^2_{41} with $s^2_{23} \in (0.433, 0.545)$ and $\Delta m^2_{41} \in (10.0, 30.0)10^6$ meV^2 is depicted in Fig. 8. The dependences of the absolute values of the entries of the lepton mixing matrix in Eq. (28) on s_{13} and s_{23} are presented in Figs. C1 and D1, which

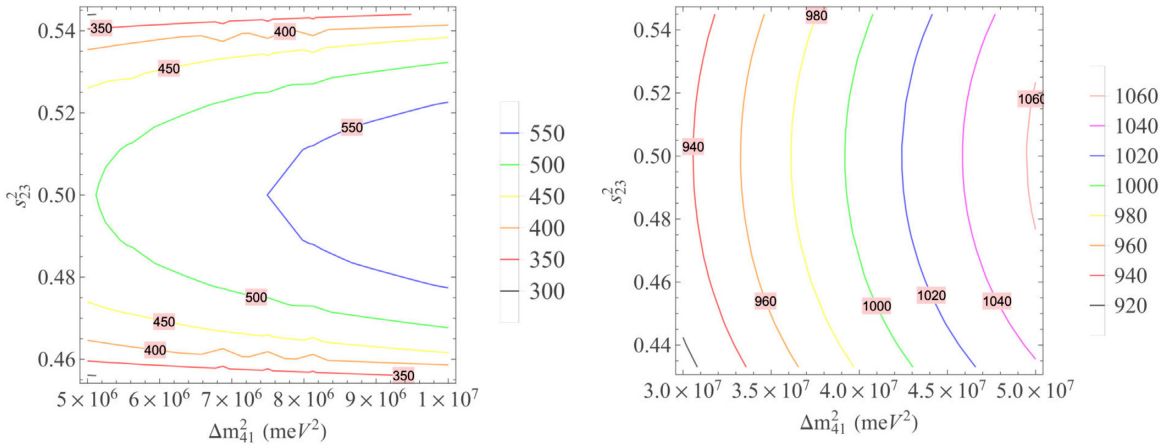

Fig. 9. m_β (meV) as a function of s^2_{23} and s^2_{13} with $s^2_{23} \in (0.456, 0.544)$ and $\Delta m^2_{41} \in (5.0, 10.0)10^6\,\text{meV}^2$ for NH (in the left panel) and $s^2_{23} \in (0.433, 0.545)$ and $\Delta m^2_{41} \in (30.0, 50.0)10^6\,\text{meV}^2$ for IH (in the right panel).

indicate that

$$|U_{\text{lep}}| \in \begin{cases} \begin{pmatrix} 0.8020 \to 0.8040 & \frac{1}{\sqrt{3}} & 0.142 \to 0.154 \\ 0.370 \to 0.420 & \frac{1}{\sqrt{3}} & 0.700 \to 0.730 \\ 0.430 \to 0.470 & \frac{1}{\sqrt{3}} & 0.670 \to 0.695 \end{pmatrix} & \text{for NH,} \\ \begin{pmatrix} 0.8020 \to 0.8040 & \frac{1}{\sqrt{3}} & 0.144 \to 0.154 \\ 0.440 \to 0.490 & \frac{1}{\sqrt{3}} & 0.655 \to 0.690 \\ 0.340 \to 0.400 & \frac{1}{\sqrt{3}} & 0.710 \to 0.745 \end{pmatrix} & \text{for IH.} \end{cases} \tag{67}$$

At the best-fit points of the two light neutrino mass-squared differences and the reactor neutrino mixing angle taken from Ref. [45], $\Delta m^2_{31} = 75.0\,\text{meV}^2$ and $\Delta m^2_{31} = 2.55 \times 10^3\,\text{meV}^2$, $s^2_{13} = 2.200 \times 10^{-2}$ for NH and $\Delta m^2_{31} = -2.45 \times 10^3\,\text{meV}^2$, $s^2_{13} = 2.225 \times 10^{-2}$for IH, the parameter m_β and $s^2_{k4}\,(k = 1, 2, 3)$ depend on s_{23} and $m_s = \sqrt{\Delta m^2_{14}}$. At present, there are various experimental bounds on Δm^2_{41} [6–12,76–81], e.g., $\Delta m^2_{41} \in (0.01, 1.0)\,\text{eV}^2$ [76], $\Delta m^2_{41} > 10^{-2}\,\text{eV}^2$ [8], $\Delta m^2_{41} = 0.041\,\text{eV}^2$ [78], $\Delta m^2_{41} \in (0.1, 1.0)\,\text{eV}^2$ [77], $\Delta m^2_{41} \in (0.2, 10.0)\,\text{eV}^2$ [9], $\Delta m^2_{41} \geq 0.1\,\text{eV}^2$ [10], $\Delta m^2_{41} = 1.0\,\text{eV}^2$ [79,80], $\Delta m^2_{41} > 1.5\,\text{eV}^2$ [11], $\Delta m^2_{41} = 1.7\,\text{eV}^2$ [81], $\Delta m^2_{41} < 10.0\,\text{eV}^2$ [6], and $\Delta m^2_{41} = 1.45\,\text{eV}^2$ [7]. Thus in this work, Δm^2_{41} is assumed to be in the range of $\Delta m^2_{41} \in (5.0, 10)\,\text{eV}^2$ for NH and of $\Delta m^2_{41} \in (30.0, 50.0)\,\text{eV}^2$ for IH. Going by this assumption, the dependences of m_β and s^2_{k4} on s_{23} and Δm^2_{41}, with $s^2_{23} \in (0.456, 0.544)$ and $\Delta m^2_{41} \in (5.0, 10.0)10^6\,\text{meV}^2$ for NH and $s^2_{23} \in (0.433, 0.545)$ and $\Delta m^2_{41} \in (30, 50)10^6\,\text{meV}^2$ for IH, are presented in Figs. 9, 10, and 11, respectively.

Figures 10 and 11 show that the considered model predicts the ranges of s^2_{14}, s^2_{24}, and s^2_{34} as follows:

$$s^2_{14} \in \begin{cases} (0.015,\ 0.045) & \text{for NH,} \\ (0.022,\ 0.029) & \text{for IH,} \end{cases} \tag{68}$$

$$s^2_{24} \in \begin{cases} (0.005,\ 0.012) & \text{for NH,} \\ (0.0095,\ 0.012) & \text{for IH,} \end{cases} \tag{69}$$

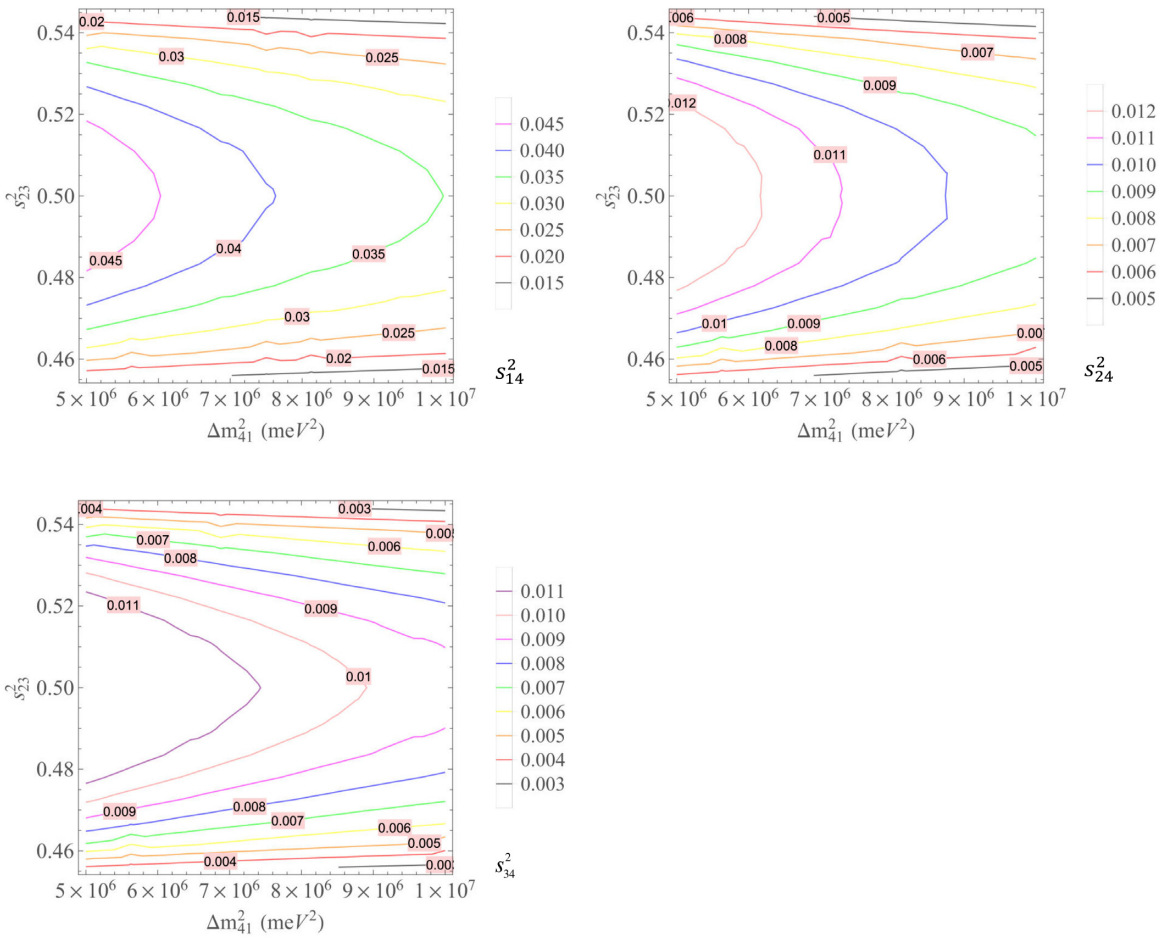

Fig. 10. s_{14}^2, s_{24}^2, and s_{34}^2 as functions of s_{23}^2 and Δm_{41}^2 with $s_{23}^2 \in (0.456, 0.544)$ and $\Delta m_{41}^2 \in (5.0, 10.0)10^6$ meV^2 for NH.

$$s_{34}^2 \in \begin{cases} (0.003,\ 0.011) & \text{for} \quad \text{NH}, \\ (0.009,\ 0.012) & \text{for} \quad \text{IH}, \end{cases} \tag{70}$$

which are consistent with the constraints given in Table 1.

Finally, from the above analysis, the obtained parameters of the model are summarized in Table 3. In the case of $s_{23}^2 = 0.544\,(\theta_{23} = 47.50^\circ)$ and $\Delta m_{41}^2 = 5.0\,\text{eV}^2$ for NH and $s_{23}^2 = 0.545\,(\theta_{23} = 47.58^\circ)$ and $\Delta m_{41}^2 = 30.0\,\text{eV}^2$ ($m_s = 4477.23$ meV) for IH, we obtain the parameters as given in Table 4 and the lepton mixing matrix gets the explicit form:

$$U_{\text{lep}} = \begin{cases} \begin{pmatrix} 0.8012 + 0.052\,87i & 0.5774 & -0.1285 - 0.074\,06i \\ 0.096\,36 - 0.354i & -0.2887 + 0.5i & -0.6317 - 0.3646i \\ 0.096\,36 + 0.4598i & -0.2887 - 0.5i & -0.6317 + 0.2165i \end{pmatrix} & \text{for} \quad \text{NH}, \\ \begin{pmatrix} 0.8009 - 0.054\,05i & 0.5774 & -0.1285 + 0.075\,75i \\ 0.095\,96 - 0.4611i & -0.288 + 0.5i & -0.6315 - 0.2147i \\ 0.095\,96 + 0.353i & -0.2888 - 0.5i & -0.6315 + 0.3662i \end{pmatrix} & \text{for} \quad \text{IH}, \end{cases} \tag{71}$$

which are unitary and in good agreement with the constraint on the absolute values of the entries of the lepton mixing matrix given in Eq. (1).

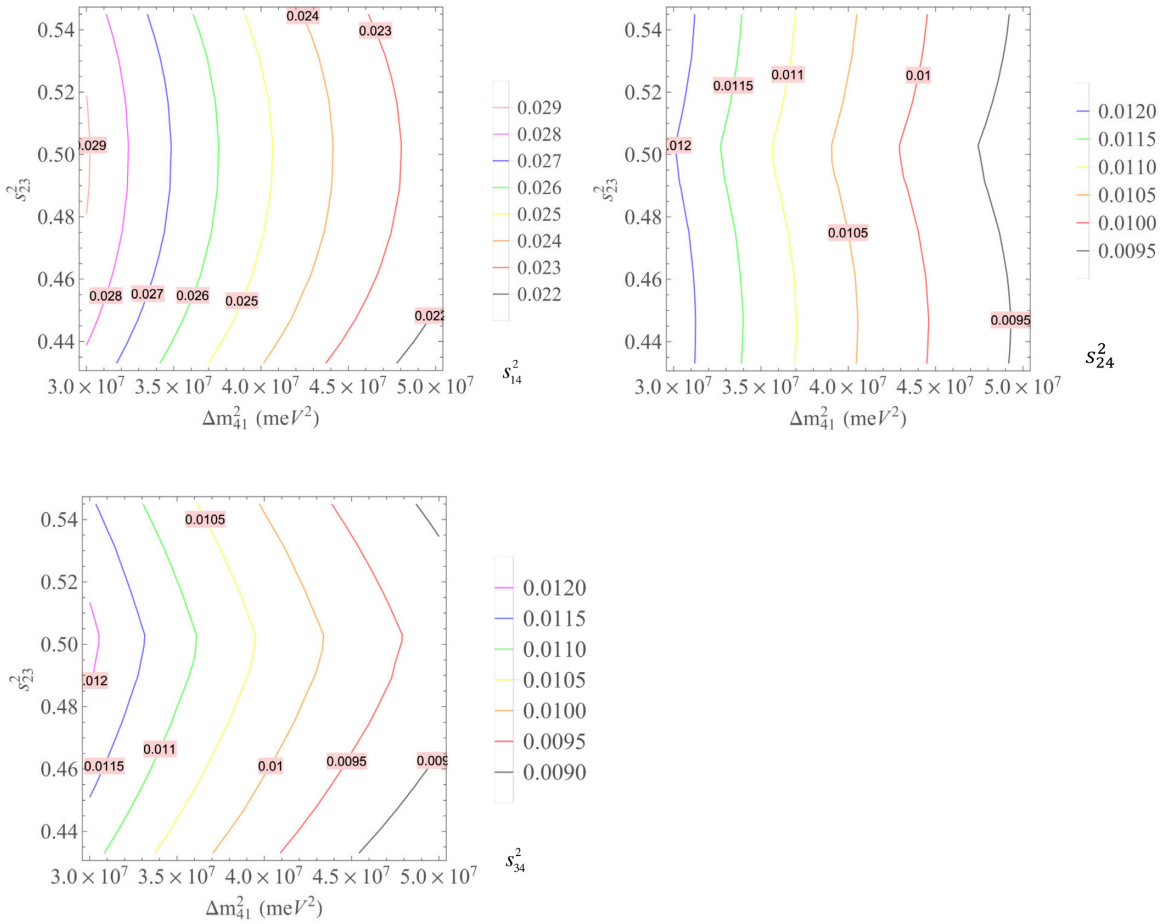

Fig. 11. s^2_{14}, s^2_{24}, and s^2_{34} as functions of s^2_{23} and Δm^2_{41} with $s^2_{23} \in (0.433, 0.545)$ and $\Delta m^2_{41} \in (30.0, 50.0)10^6\,\text{meV}^2$ for IH.

4. Muon anomalous magnetic moment

The experimental data show a significant deviation of the muon anomalous magnetic moment from its SM value:

$$\Delta a_\mu = a_\mu^{\text{exp}} - a_\mu^{\text{SM}} = (2.51 \pm 0.59) \times 10^{-9}. \tag{72}$$

In this subsection, we will analyze the implications of our model in the muon anomalous magnetic moment. Muon anomalous magnetic moments mainly arise from one-loop diagrams involving the exchange of electrically neutral *CP*-even and *CP*-odd scalars and the muon running in the internal lines of the loop. It is worth mentioning that due to the symmetries in our model, there are no tree-level flavor-changing neutral scalar interactions in the leptonic Yukawa terms, thus implying that the muon is the only charged lepton contributing to the muon anomalous magnetic moment. There are also contributions arising from electrically charged scalar and right-handed Majorana neutrinos but these contributions are strongly suppressed. Thus, the leading contributions to the muon anomalous magnetic moment take the form:

$$\begin{aligned}\Delta a_\mu \simeq & \frac{\left[\left(y_{h\overline{\mu}_R\mu_L}\right)^2 - \left(y^{(SM)}_{h\overline{\mu}_R\mu_L}\right)^2\right] m_\mu^2}{8\pi^2} I_H^{(\mu)}\left(m_\mu, m_h\right) \\ & + \frac{m_\mu^2}{8\pi^2}\left[y^2_{H^0\overline{\mu}_R\mu_L} I_H^{(\mu)}\left(m_\mu, m_{H^0}\right) + y^2_{A^0\overline{\mu}_R\mu_L} I_A^{(\mu)}\left(m_\mu, m_{A^0}\right)\right],\end{aligned} \tag{73}$$

Table 3. The model prediction compared to the experimental range [45,46].

Parameters	Experimental range (NH)	Prediction (NH)	Experimental range (IH)	Prediction (IH)
$\sum_{i=1}^{3} m_i$ (meV)	<120	58.03 → 60.31	<150	98.07 → 101.30
$\sin^2\theta_{13} \times 10^2$	2.00 → 2.405	2.00 → 2.405	2.018 → 2.424	2.018 → 2.424
$\sin^2\theta_{12}$	0.271 → 0.369	0.3401 → 0.3415	0.271 → 0.369	0.3402 → 0.3416
$\sin^2\theta_{23}$	0.434 → 0.610	0.456 → 0.544	0.433 → 0.608	0.433 → 0.545
δ_{CP} (°)	128 → 352	156 → 172	200 → 353	140.8 → 167.2
s_{14}^2	0.0098 → 0.0310	0.015 → 0.045	0.0098 → 0.0310	0.022 → 0.029
s_{24}^2	0.0059 → 0.0262	0.005 → 0.012	0.0059 → 0.0262	0.0095 → 0.012
s_{34}^2	0 → 0.0369	0.003 → 0.011	0 → 0.0369	0.009 → 0.012
$\langle m_{ee}^{(3)} \rangle$ (meV)	≈1.0 [95]	3.50 → 4.1	≈1.0 [95]	47.90 → 48.50
$m_\beta^{(3)}$ (meV)	8.9 → 12.6 [95]	8.85 → 9.15	8.9 → 12.6 [95]	47.17 → 49.23
$\langle m_{ee} \rangle$ (meV)	< 110 → 520 [74]	40.0 → 110.0	<110 → 520 [74]	185.0 → 205.0
m_β (meV)	<1100 [96]	300.0 → 550.0	<1100 [96]	700.0 → 900.0

Table 4. The obtained parameters.

Parameters	Derived values (NH)	Derived values (IH)
k_2	−2.29	1.161
k_3	0.439	0.9758
$\cos\alpha$ $\left(\alpha^{(\circ)}\right)$	−0.136 (97.80)	0.9758 (4.412)
k_0	5.83	0.985
m_1 (meV)	0	49.50
m_2 (meV)	8.66	50.25
m_1 (meV)	50.50	0
$\sum_{i=1}^{3} m_i$ (meV)	59.20	99.75
$\sin\delta_{CP}$ $\left(\delta_{CP}^{(\circ)}\right)$	−0.912 (294.0)	−0.9092 (294.60)
m_s (eV)	2.24	4.472
s_{14}^2	0.0178	0.028 53
s_{24}^2	0.005 89	0.012 25
s_{34}^2	0.003 94	0.011 57
$\langle m_{ee}^{(3)} \rangle$ (meV)	3.575	48.45
$\langle m_{ee} \rangle$ (meV)	37.27	203.90
$m_\beta^{(3)}$ (meV)	9.006	49.20
m_β (meV)	294.20	926.40

where the Yukawa couplings appearing in Eq. (73) are given by:

$$y_{h\overline{\mu}_R\mu_L} = \sqrt{\frac{3}{2}}\left(y_2 \sin\alpha - y_3 \cos\alpha\right), \qquad y_{h\overline{\mu}_R\mu_L}^{(SM)} = \frac{m_\mu}{v}, \tag{74}$$

$$y_{H^0\overline{\mu}_R\mu_L} = \sqrt{\frac{3}{2}}\left(y_2 \cos\alpha + y_3 \sin\alpha\right), \qquad y_{A^0\overline{\mu}_R\mu_L} = \sqrt{\frac{3}{2}}\left(y_2 \sin\beta - y_3 \cos\beta\right), \tag{75}$$

whereas the loop function $I_{H(A)}^{(\mu)}\left(m_f, m_{H,A}\right)$ has the form [90–94]:

$$I_{H(A)}^{(\mu)}\left(m_f, m_{H,A}\right) = \int_0^1 \frac{x^2\left(1 - x \pm \frac{m_f}{m_\mu}\right)}{m_\mu^2 x^2 + \left(m_f^2 - m_\mu^2\right)x + m_{H,A}^2\left(1 - x\right)} dx. \tag{76}$$

Figure 12 shows the allowed parameter space in the m_{H^0}–m_{A^0} plane consistent with the muon

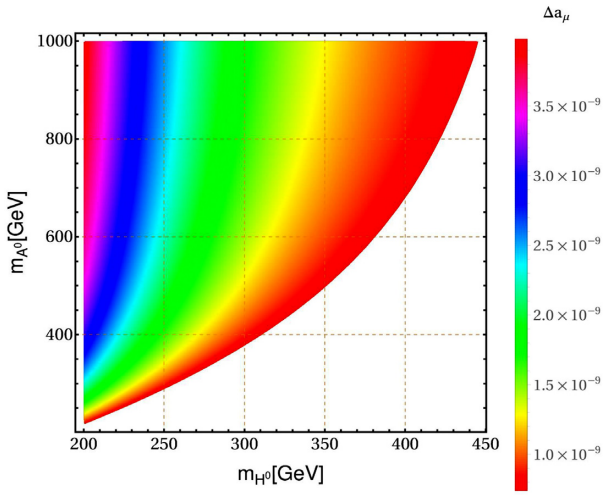

Fig. 12. Allowed parameter space in the m_{H^0}–m_{A^0} plane consistent with the muon anomalous magnetic moment. We find that our model can successfully accommodate the experimental values of the muon anomalous magnetic moment.

5. Conclusions

We have proposed a $B - L$ model combined with the $S_4 \times Z_3 \times Z_4$ discrete group that successfully explains the recent 3+1 sterile–active neutrino data. The tiny masses of the light active neutrinos are obtained through the type-I seesaw mechanism. The active–active and sterile–active neutrino mixing angles are predicted to be consistent with the recent constraints where $0.3401\,(0.3402) \leq \sin^2\theta_{12} \leq 0.3415\,(0.3416)$, $0.456\,(0.433) \leq \sin^2\theta_{23} \leq 0.544\,(0.545)$, $2.00\,(2.018) \leq 10^2 \times \sin^2\theta_{13} \leq 2.405\,(2.424)$, $156\,(140.8) \leq \delta_{CP}^{(\circ)} \leq 172\,(167.2)$ for normal (inverted) ordering of the three-neutrino scenario, and $0.015\,(0.022) \leq s_{14}^2 \leq 0.045\,(0.029)$, $0.005(0.0095) \leq s_{24}^2 \leq 0.012\,(0.012)$, $0.003\,(0.009) \leq s_{34}^2 \leq 0.011$ for normal (inverted) ordering of the 3+1 neutrino scenario. The effective neutrino masses are predicted to be in the ranges $40.0\,(185) \leq \langle m_{ee}\rangle[\text{meV}] \leq 110.0\,(205.0)$ and $300\,(700) \leq \langle m_\beta\rangle[\text{meV}] \leq 550\,(900)$ for normal and inverted neutrino mass orderings, respectively, a range of values consistent with the recent experimental data. Our model predicts flavor-conserving leptonic neutral scalar interactions and successfully explains the muon $g - 2$ anomaly.

Acknowledgments

A.E.C.H. is supported by ANID-Chile FONDECYT 1210378, ANID PIA/APOYO AFB180002, and ANID- Programa Milenio, code ICN2019_044. H.N.L. acknowledges the financial support of the International Center of Physics at the Institute of Physics, VAST under grant No. ICP.2022.02.

Appendix A. Interactions are prevented by one of the symmetries of the model

Appendix B. Higgs potential invariant under Γ symmetry

The total renormalizable scalar potential invariant under Γ symmetry is given by[4]:

$$\begin{aligned} V_{\text{scal}} = {} & V(H) + V(H') + V(\phi) + V(\varphi) + V(\rho) + V(\chi) + V(\phi_s) + V(HH') + V(H\phi) \\ & + V(H\varphi) + V(H\rho) + V(H\chi) + V(H\phi_s) + V(H'\phi) + V(H'\varphi) + V(H'\rho) + V(H'\chi) \\ & + V(H'\phi_s) + V(\phi\varphi) + V(\phi\rho) + V(\phi\chi) + V(\phi\phi_s) + V(\varphi\rho) + V(\varphi\chi) + V(\varphi\phi_s) \\ & + V(\rho\chi) + V(\rho\phi_s) + V(\chi\phi_s) + V_{\text{trip}} + V_{\text{quart}}, \end{aligned} \tag{B1}$$

[4]Here, $V(a_1 \to a_2, b_1 \to b_2, \cdots) \equiv V(a_1, b_1, \cdots)_{\{a_1=a_2,\, b_1=b_2, \cdots\}}$.

Table A1. Forbidden terms.

Couplings	**Forbidden by**
$(\overline{\psi}_L\psi_L^c)_{\mathbf{1}}\widetilde{H}^2$, $(\overline{\psi}_L\psi_L^c)_{\mathbf{1}}\widetilde{H'}^2$, $(\overline{\nu}_R^C\nu_R)_{\mathbf{1}}(\chi^{*2})_{\mathbf{1}}$, $(\overline{\nu}_R^C\nu_R)_{\mathbf{1}}(\phi\varphi^*)_{\mathbf{1}}$, $(\overline{\nu}_R^C\nu_R)_{\mathbf{2}}(\phi\varphi^*)_{\mathbf{2}}$, $(\overline{\nu}_R^C\nu_R)_{\mathbf{3}}(\phi\varphi^*)_{\mathbf{3}}$, $(\overline{\nu}_R^C\nu_R)_{\mathbf{3}'}(\phi\varphi^*)_{\mathbf{3}'}$, $(\overline{\nu}_R^C\nu_R)_{\mathbf{3}}(\phi\rho^*)_{\mathbf{3}}$, $(\overline{\nu}_R^C\nu_R)_{\mathbf{1}}(\phi^*\phi_s)_{\mathbf{1}}$, $(\overline{\nu}_R^C\nu_R)_{\mathbf{2}}(\phi^*\phi_s)_{\mathbf{2}}$, $(\overline{\nu}_R^C\nu_R)_{\mathbf{3}}(\phi^*\phi_s)_{\mathbf{3}}$, $(\overline{\nu}_R^C\nu_R)_{\mathbf{3}'}(\phi^*\phi_s)_{\mathbf{3}'}$, $(\overline{\nu}_R^C\nu_R)_{\mathbf{1}}(\varphi\phi_s^*)_{\mathbf{1}}$, $(\overline{\nu}_R^C\nu_R)_{\mathbf{2}}(\varphi\phi_s^*)_{\mathbf{2}}$, $(\overline{\nu}_R^C\nu_R)_{\mathbf{3}}(\varphi\phi_s^*)_{\mathbf{3}}$, $(\overline{\nu}_R^C\nu_R)_{\mathbf{3}'}(\varphi\phi_s^*)_{\mathbf{3}'}$, $(\overline{\nu}_R^C\nu_R)_{\mathbf{1}}(\rho\phi_s^*)_{\mathbf{1}}$, $(\overline{\nu}_s^C\nu_R)_{\mathbf{3}}\varphi$, $(\overline{\nu}_s^C\nu_R)_{\mathbf{3}}(\phi\chi^*)_{\mathbf{3}}$, $(\overline{\nu}_s^C\nu_s)_{\mathbf{1}}(\phi^2)_{\mathbf{1}}$, $(\overline{\nu}_s^C\nu_s)_{\mathbf{1}}(\phi_s^{*2})_{\mathbf{1}}$, $(\overline{\nu}_s^C\nu_s)_{\mathbf{1}}(\phi^*\varphi^*)_{\mathbf{1}}$, $(\overline{\nu}_s^C\nu_s)_{\mathbf{1}}(\varphi\phi_s)_{\mathbf{1}}$.	$\boldsymbol{U(1)_{B-L}}$
$(\overline{\psi}_L l_{1R})_{\mathbf{3}}(H'\phi)_{\mathbf{3}'}$, $(\overline{\psi}_L\nu_R)_{\mathbf{1}}(\widetilde{H}'\rho)_{\mathbf{1}'}$.	$\boldsymbol{S_4}$
$(\overline{\psi}_L l_{1R})_{\mathbf{3}}(H\varphi)_{\mathbf{3}}$, $(\overline{\psi}_L l_{1R})_{\mathbf{3}}(H\phi_s)_{\mathbf{3}}$, $(\overline{\psi}_L l_{\alpha R})_{\mathbf{3}}(H\varphi)_{\mathbf{3}}$, $(\overline{\psi}_L l_{\alpha R})_{\mathbf{3}}(H\phi_s)_{\mathbf{3}}$, $(\overline{\psi}_L l_{\alpha R})_{\mathbf{3}}(H'\varphi)_{\mathbf{3}'}$, $(\overline{\psi}_L l_{\alpha R})_{\mathbf{3}}(H'\phi_s)_{\mathbf{3}'}$, $(\overline{\psi}_L\nu_R)_{\mathbf{3}}(\widetilde{H}\phi)_{\mathbf{3}}$, $(\overline{\psi}_L\nu_R)_{\mathbf{3}}(\widetilde{H}\phi_s)_{\mathbf{3}}$, $(\overline{\psi}_L\nu_R)_{\mathbf{3}'}(\widetilde{H}'\phi)_{\mathbf{3}'}$, $(\overline{\psi}_L\nu_R)_{\mathbf{3}'}(\widetilde{H}'\phi_s)_{\mathbf{3}'}$, $(\overline{\nu}_s^C\nu_R)_{\mathbf{3}}(\phi\chi)_{\mathbf{3}}$, $(\overline{\nu}_s^C\nu_R)_{\mathbf{3}}(\varphi\chi)_{\mathbf{3}}$.	$\boldsymbol{Z_3}$
$(\overline{\psi}_L l_{\alpha R})_{\mathbf{3}}(H'\phi_s^*)_{\mathbf{3}'}$, $(\overline{\psi}_L\nu_R)_{\mathbf{1}}\widetilde{H}$, $(\overline{\psi}_L\nu_R)_{\mathbf{3}}(\widetilde{H}\varphi^*)_{\mathbf{3}}$, $(\overline{\psi}_L\nu_R)_{\mathbf{1}}(\widetilde{H}\rho^*)_{\mathbf{1}}$, $(\overline{\psi}_L\nu_R)_{\mathbf{3}'}(\widetilde{H}'\varphi^*)_{\mathbf{3}'}$, $(\overline{\psi}_L\nu_s)_{\mathbf{3}}(\widetilde{H}\phi^*)_{\mathbf{3}}$, $(\overline{\psi}_L\nu_s)_{\mathbf{3}}(\widetilde{H}\phi_s)_{\mathbf{3}}$, $(\overline{\nu}_R^C\nu_R)_{\mathbf{3}}(\varphi\chi)_{\mathbf{3}}$, $(\overline{\nu}_R^C\nu_R)_{\mathbf{3}}(\varphi^*\chi)_{\mathbf{3}}$, $(\overline{\nu}_R^C\nu_R)_{\mathbf{1}}(\rho\chi)_{\mathbf{1}}$, $(\overline{\nu}_R^C\nu_R)_{\mathbf{1}}(\rho^*\chi)_{\mathbf{1}}$, $(\overline{\nu}_s^C\nu_R)_{\mathbf{3}}(\phi^*\chi)_{\mathbf{3}}$.	$\boldsymbol{Z_4}$

where

$$
\begin{aligned}
V(H) &= \mu_H^2 H^\dagger H + \lambda^H (H^\dagger H)^2,\ V(H') = V(H, H \to H'),\\
V(\phi) &= \mu_\phi^2 \phi^*\phi + \lambda_1^\phi(\phi^*\phi)_1(\phi^*\phi)_1 + \lambda_2^\phi(\phi^*\phi)_2(\phi^*\phi)_2 + \lambda_3^\phi(\phi^*\phi)_3(\phi^*\phi)_3 + \lambda_4^\phi(\phi^*\phi)_{3'}(\phi^*\phi)_{3'},\\
V(\varphi) &= V(\phi \to \varphi),\ V(\rho) = \mu_\rho^2\rho^*\rho + \lambda^\rho(\rho^*\rho)_1(\rho^*\rho)_1,\ V(\chi) = V(\rho \to \chi),\ V(\phi_s) = V(\phi \to \phi_s),\\
V(H, H') &= \lambda_1^{HH'}(H^\dagger H)_1(H'^\dagger H')_1 + \lambda_2^{HH'}(H^\dagger H')_{1'}(H'^\dagger H)_{1'},\ V(H, \phi) = \lambda_1^{H\phi}(H^\dagger H)_1(\phi^*\phi)_1\\
&\quad + \lambda_2^{H\phi}(H^\dagger\phi)_3(\phi^* H)_3,\ V(H, \varphi) = V(H, \phi \to \varphi),\ V(H, \rho) = \lambda_1^{H\rho}(H^\dagger H)_1(\rho^*\rho)_1\\
&\quad + \lambda_2^{H\rho}(H^\dagger\rho)_1(\rho^* H)_1,\ V(H, \chi) = V(H, \rho \to \chi),\ \ V(H, \phi_s) = V(H, \phi \to \phi_s),\\
V(H, H') &= \lambda_1^{HH'}(H^\dagger H)_1(H'^\dagger H')_1 + \lambda_2^{HH'}(H^\dagger H')_{1'}(H'^\dagger H)_{1'},\ V(H, \phi) = \lambda_1^{H\phi}(H^\dagger H)_1(\phi^*\phi)_1\\
&\quad + \lambda_2^{H\phi}(H^\dagger\phi)_3(\phi^* H)_3,\ V(H, \varphi) = V(H, \phi \to \varphi),\ V(H, \rho) = \lambda_1^{H\rho}(H^\dagger H)_1(\rho^*\rho)_1\\
&\quad + \lambda_2^{H\rho}(H^\dagger\rho)_1(\rho^* H)_1,\ V(H, \chi) = V(H, \rho \to \chi),\ \ V(H, \phi_s) = V(H, \phi \to \phi_s),\\
V(H', \phi) &= \lambda_1^{H'\phi}(H'^\dagger H')_1(\phi^*\phi)_1 + \lambda_2^{H'\phi}(H'^\dagger\phi)_{3'}(\phi^* H')_{3'},\ V(H', \varphi) = V(H', \phi \to \varphi),\\
V(H', \rho) &= \lambda_1^{H'\rho}(H'^\dagger H')_1(\rho^*\rho)_1 + \lambda_2^{H'\rho}(H'^\dagger\rho)_{1'}(\rho^* H')_{1'},\ V(H', \chi) = V(H', \rho \to \chi),\\
V(H', \phi_s) &= V(H', \phi \to \phi_s),\ V(\phi, \rho) = \lambda_1^{\phi\rho}(\phi^*\phi)_1(\rho^*\rho)_1 + \lambda_2^{\phi\rho}(\phi^*\rho)_3(\rho^*\phi)_3,\\
V(\phi, \chi) &= V(\phi, \rho \to \chi),\ V(\phi, \varphi) = \lambda_1^{\phi\varphi}(\phi^*\phi)_1(\varphi^*\varphi)_1 + \lambda_2^{\phi\varphi}(\phi^*\phi)_2(\varphi^*\varphi)_2 + \lambda_3^{\phi\varphi}(\phi^*\phi)_3(\varphi^*\varphi)_3\\
&\quad + \lambda_4^{\phi\varphi}(\phi^*\phi)_{3'}(\varphi^*\varphi)_{3'} + \lambda_5^{\phi\varphi}(\phi^*\varphi)_1(\varphi^*\phi)_1 + \lambda_6^{\phi\varphi}(\phi^*\varphi)_2(\varphi^*\phi)_2 + \lambda_7^{\phi\varphi}(\phi^*\varphi)_3(\varphi^*\phi)_3\\
&\quad + \lambda_8^{\phi\varphi}(\phi^*\varphi)_{3'}(\varphi^*\phi)_{3'},\ V(\phi, \phi_s) = V(\phi, \varphi \to \phi_s),\ V(\varphi, \chi) = V(\phi \to \varphi, \chi),\\
V(\varphi, \phi_s) &= V(\phi \to \varphi, \phi_s),\ V(\rho, \chi) = \lambda_1^{\rho\chi}(\rho^*\rho)_1(\chi^*\chi)_1 + \lambda_2^{\rho\chi}(\rho^*\chi)_1(\chi^*\rho)_1,\\
V(\rho, \phi_s) &= V(H \to \rho, \phi \to \phi_s),\ V(\chi, \phi_s) = V(\rho \to \chi, \phi_s),\\
V_{\rm trip} &= \lambda_1^{\phi\varphi\rho}(\phi^*\phi)_3(\varphi^*\rho)_3 + \lambda_2^{\phi\varphi\rho}(\phi^*\phi)_3(\varphi\rho^*)_3 + \lambda_3^{\phi\varphi\rho}(\phi^*\rho)_3(\varphi^*\phi)_3 + \lambda_4^{\phi\varphi\rho}(\phi^*\varphi)_3(\phi\rho^*)_3,\\
V_{\rm quart} &= \lambda_1^{\phi\varphi\rho\phi_s}(\phi\varphi)_3(\rho\phi_s)_3 + \lambda_2^{\phi\varphi\rho\phi_s}(\phi\phi_s)_3(\rho\varphi)_3 + \lambda_3^{\phi\varphi\rho\phi_s}(\phi_s\varphi)_3(\rho\phi)_3\\
&\quad + \lambda_4^{\phi\varphi\rho\phi_s}(\phi^*\varphi^*)_3(\rho^*\phi_s^*)_3 + \lambda_5^{\phi\varphi\rho\phi_s}(\phi^*\phi_s^*)_3(\rho^*\varphi^*)_3 + \lambda_6^{\phi\varphi\rho\phi_s}(\phi_s^*\varphi^*)_3(\rho^*\phi^*)_3. \qquad \text{(B2)}
\end{aligned}
$$

Now we show that the VEV alignments in Eq. (3) satisfy the minimization condition of the scalar potential $V_{\rm scal}$ of the model whose explicit expression is given in Eqs. (B1)–(B2). For this

purpose we suppose that the VEVs of the scalars H, $H^{'}$, ϕ, ρ, χ, and ϕ_s are real while that of φ is complex, i.e., $v^* = v$, $v^{'*} = v'$, $v_\phi^* = v_\phi$, $v_\rho^* = v_\rho$, $v_\chi^* = v_\chi$, $v_{\phi_s}^* = v_{\phi_s}$, and $v_\varphi = v_0 e^{i\alpha}$. The minimization condition of $V_{\rm scal}$ reads

$$\frac{\partial V_{\rm scal}}{\partial v_\lambda} = 0,\ \delta_\lambda^2 \sim \frac{\partial^2 V_{\rm scal}}{\partial v_\lambda^2} > 0\ (v_\lambda = v,\ v',\ v_\phi,\ v_\rho,\ v_\chi,\ v_{\phi_s},\ v_0,\ \alpha). \tag{B3}$$

For simplicity we will work with the following benchmark points:

$$\begin{aligned}
&\lambda_1^{H\varphi} = \lambda_2^{H\varphi} = \lambda_1^{H'\varphi} = \lambda_2^{H'\varphi} = \lambda_1^{H\chi} = \lambda_2^{H\chi} = \lambda_1^{H'\chi} = \lambda_2^{H'\chi} = \lambda_1^{HH'} = \lambda_2^{HH'} \\
&= \lambda_1^{H\phi} = \lambda_2^{H\phi} = \lambda_1^{H'\phi} = \lambda_2^{H'\phi} = \lambda_1^{H\rho} = \lambda_2^{H\rho} = \lambda_1^{H'\rho} = \lambda_2^{H'\rho} = \lambda_1^{H\phi_s} = \lambda_2^{H\phi_s} \\
&= \lambda_1^{H'\phi_s} = \lambda_2^{H'\phi_s} = \lambda_1^{\phi\chi} = \lambda_2^{\phi\chi} = \lambda_1^{\phi\varphi} = \lambda_5^{\phi\varphi} = \lambda_6^{\phi\varphi} = \lambda_7^{\phi\varphi} = \lambda_8^{\phi\varphi} = \lambda_1^{H'\phi} = \lambda_2^{H'\phi} \\
&= \lambda_1^{\phi\rho} = \lambda_2^{\phi\rho} = \lambda_1^{\phi\phi_s} = \lambda_3^{\phi\phi_s} = \lambda_5^{\phi\phi_s} = \lambda_6^{\phi\phi_s} = \lambda_7^{\phi\phi_s} = \lambda_8^{\phi\phi_s} = \lambda_1^{\varphi\chi} = \lambda_2^{\varphi\chi} = \lambda_1^{\varphi\rho} \\
&= \lambda_2^{\varphi\rho} = \lambda_1^{\rho\chi} = \lambda_2^{\rho\chi} = \lambda_1^{\rho\phi_s} = \lambda_2^{\rho\phi_s} = \lambda_1^{H\chi} = \lambda_2^{H\chi} = \lambda_1^{\chi\phi_s} = \lambda_2^{\chi\phi_s} = \lambda_1^{\varphi\phi_s} = \lambda_2^{\varphi\phi_s} \\
&= \lambda_7^{\varphi\phi_s} = \lambda_8^{\varphi\phi_s} = \lambda_3^{\phi\varphi\rho\phi_s} = \lambda_2^{\phi\varphi\rho\phi_s} = \lambda_1^{\phi\varphi\rho\phi_s} = \lambda_3^{\phi\varphi\rho} = \lambda_1^{\phi\varphi\rho} = \lambda^x,
\end{aligned} \tag{B4}$$

$$\lambda_6^{\phi\varphi\rho\phi_s} = \lambda_5^{\phi\varphi\rho\phi_s} = \lambda_4^{\phi\varphi\rho\phi_s} = a\lambda_1^{\phi\varphi\rho\phi_s} = a\lambda^x,\ \lambda_4^{\phi\varphi\rho} = \lambda_2^{\phi\varphi\rho} = a\lambda^x, \tag{B5}$$

$$\lambda_1^{\phi} = \lambda_3^{\phi} = \lambda^{\phi},\ \lambda_1^{\varphi} = \lambda_2^{\varphi} = \lambda^{\varphi},\ \lambda_1^{\phi_s} = \lambda_2^{\phi_s} = \lambda_3^{\phi_s} = \lambda^{\phi_s}. \tag{B6}$$

As a consequence, the condition (B3) becomes

$$\mu_H^2 + 2\lambda^H v^2 + 2\lambda^x \left(v_\varphi^2 + v_\chi^2 + v'^2 + 3v_\phi^2 + v_\rho^2 + 2v_s^2\right) = 0, \tag{B7}$$

$$\mu_{H'}^2 + 2\lambda^{H'} v'^2 + 2\lambda^x \left(v^2 + v_\varphi^2 + v_\chi^2 + 3v_\phi^2 + v_\rho^2 + 2v_s^2\right) = 0, \tag{B8}$$

$$\begin{aligned}
&6\mu_\phi^2 v_\phi + 84\lambda^\phi v_\phi^3 + 2\lambda^x \Big[6v_\phi \left(v^2 + v_\varphi^2 + v_\chi^2 + v'^2 + v_\rho^2\right) + 20v_\phi v_s^2 + e^{i\alpha} v_\varphi v_\rho \left(4av_\phi + 3v_s\right) \\
&+ e^{-i\alpha} v_\varphi v_\rho \left(4v_\phi + 3av_s\right)\Big] = 0,
\end{aligned} \tag{B9}$$

$$\begin{aligned}
&\mu_\varphi^2 v_\varphi + 6\lambda^\varphi v_\varphi^3 + \lambda^x \Big[2v_\varphi \left(v^2 + v_\chi^2 + v'^2 + 3v_\phi^2 + v_\rho^2\right) + e^{i\alpha} v_\phi v_\rho \left(2av_\phi + 3v_s\right) \\
&+ e^{-i\alpha} v_\phi v_\rho \left(2v_\phi + 3av_s\right)\Big] = 0,
\end{aligned} \tag{B10}$$

$$\begin{aligned}
&v_\rho \left[\mu_\rho^2 + 2\lambda^\rho v_\rho^2 + 2\lambda^x \left(v^2 + v_\varphi^2 + v_\chi^2 + v'^2 + 3v_\phi^2 + 2v_s^2\right)\right] + e^{i\alpha} \lambda^x v_\varphi v_\phi \left(2av_\phi + 3v_s\right) \\
&+ e^{-i\alpha} \lambda^x v_\varphi v_\phi \left(2v_\phi + 3av_s\right) = 0,
\end{aligned} \tag{B11}$$

$$\mu_\chi^2 + 2\lambda^\chi v_\chi^2 + 2\lambda^x \left(v^2 + v_\varphi^2 + v'^2 + 3v_\phi^2 + v_\rho^2 + 2v_s^2\right) = 0, \tag{B12}$$

$$3\lambda^x v_\varphi v_\phi v_\rho \left(ae^{-i\alpha} + e^{i\alpha}\right) + 2v_s \left[\mu_{\phi_s}^2 + 2\lambda^x \left(v^2 + v_\chi^2 + v'^2 + 5v_\phi^2 + v_\rho^2\right) + 10\lambda^{\phi_s} v_s^2\right] = 0, \tag{B13}$$

$$e^{2i\alpha} \left(2av_\phi + 3v_s\right) - 2v_\phi - 3av_s = 0, \tag{B14}$$

$$\mu_H^2 + 6\lambda^H v^2 + 2\lambda^x \left(v_\varphi^2 + v_\chi^2 + v'^2 + 3v_\phi^2 + v_\rho^2 + 2v_s^2\right) > 0, \tag{B15}$$

$$\mu_{H'}^2 + 6\lambda^{H'} v'^2 + 2\lambda^x \left(v_\varphi^2 + v_\chi^2 + v^2 + 3v_\phi^2 + v_\rho^2 + 2v_s^2\right) > 0, \tag{B16}$$

$$3\mu_\phi^2 + 126\lambda^\phi v_\phi^2 + 4\lambda^x v_\varphi v_\rho \left(e^{-i\alpha} + be^{i\alpha}\right) + 6\lambda^x \left(v^2 + v_\varphi^2 + v_\chi^2 + v'^2 + v_\rho^2\right) + 20\lambda^x v_s^2 > 0, \tag{B17}$$

$$\mu_\varphi^2 + 18\lambda^\varphi v_\varphi^2 + 2\lambda^x \left(v^2 + v_\chi^2 + v'^2 + 3v_\phi^2 + v_\rho^2\right) > 0, \tag{B18}$$

$$\mu_\rho^2 + 6\lambda^\rho v_\rho^2 + 2\lambda^x \left(v^2 + v_\varphi^2 + v_\chi^2 + v'^2 + 3v_\phi^2 + 2v_s^2\right) > 0, \tag{B19}$$

$$\mu_\chi^2 + 6\lambda^\chi v_\chi^2 + 2\lambda^x \left(v^2 + v_\varphi^2 + v'^2 + 3v_\phi^2 + v_\rho^2 + 2v_s^2\right) > 0, \tag{B20}$$

$$\mu_{\phi_s}^2 + 2\lambda^x \left(v^2 + v_\chi^2 + v'^2 + 5v_\phi^2 + v_\rho^2\right) + 30\lambda^{\phi_s} v_s^2 > 0, \tag{B21}$$

$$-2v_\phi - 3av_s - e^{2i\alpha}\left(2av_\phi + 3v_s\right) > 0. \tag{B22}$$

The system of Eqs. (B7)–(B14) yields the following solution:

$$\begin{aligned}
\lambda^H &= -\frac{\mu_H^2 + 2\lambda^x \left(v_\varphi^2 + v_\chi^2 + v'^2 + 3v_\phi^2 + v_\rho^2 + 2v_s^2\right)}{2v^2}, \\
\lambda^{H'} &= -\frac{\mu_{H'}^2 + 2\lambda^x \left(v_\varphi^2 + v_\chi^2 + v^2 + 3v_\phi^2 + v_\rho^2 + 2v_s^2\right)}{2v'^2}, \\
\lambda^\phi &= -\frac{1}{42v_\phi^3}\Bigg[\left(3\mu_\phi^2 + 6\lambda^x v^2 + 6\lambda^x v_\varphi^2 + 6\lambda^x v_\chi^2 + 6\lambda^x v'^2 + 6\lambda^x v_\rho^2 + 20\lambda^x v_s^2\right) v_\phi \\
&\quad + \lambda^x v_\varphi v_\rho \left(\frac{\left(4av_\phi + 3v_s\right)\sqrt{2v_\phi + 3av_s}}{\sqrt{2av_\phi + 3v_s}} + \frac{\sqrt{2av_\phi + 3v_s}\left(4v_\phi + 3av_s\right)}{\sqrt{2v_\phi + 3av_s}}\right)\Bigg], \\
\lambda^\varphi &= -\frac{\mu_\varphi^2 v_\varphi + 2\lambda^x \left[v_\varphi \left(v^2 + v_\chi^2 + v'^2 + 3v_\phi^2 + v_\rho^2\right) + v_\phi v_\rho \sqrt{\left(2av_\phi + 3v_s\right)\left(2v_\phi + 3av_s\right)}\right]}{6v_\varphi^3}, \\
\lambda^\rho &= -\frac{\mu_\rho^2 v_\rho + 2\lambda^x \left[v_\rho \left(v^2 + v_\varphi^2 + v_\chi^2 + v'^2 + 3v_\phi^2 + 2v_s^2\right) + v_\varphi v_\phi \sqrt{\left(2av_\phi + 3v_s\right)\left(2v_\phi + 3av_s\right)}\right]}{2v_\rho^3}, \\
\lambda^\chi &= -\frac{\mu_\chi^2 + 2\lambda^x \left(v^2 + v_\varphi^2 + v'^2 + 3v_\phi^2 + v_\rho^2 + 2v_s^2\right)}{2v_\chi^2}, \ \alpha = i\log\left(\sqrt{\frac{2av_\phi + 3v_s}{2v_\phi + 3av_s}}\right), \\
\lambda^{\phi_s} &= -\frac{\mu_{\phi_s}^2 v_s + 2\lambda^x \left(v^2 + v_\chi^2 + v'^2 + 5v_\phi^2 + v_\rho^2\right) v_s}{10v_s^3} - \frac{3\lambda^x v_\varphi v_\phi v_\rho \left(v_\phi + a^2 v_\phi + 3av_s\right)}{10v_s^3\sqrt{\left(2av_\phi + 3v_s\right)\left(2v_\phi + 3av_s\right)}}.
\end{aligned} \tag{B23}$$

With the aid of the solution (B23), expressions (B15)–(B18) become

$$\delta_v^2 \sim -\mu_H^2 - 2\lambda^x \left(v_\varphi^2 + v_\chi^2 + v'^2 + 3v_\phi^2 + v_\rho^2 + 2v_s^2\right) > 0, \tag{B24}$$

$$\delta_{v'}^2 \sim -\mu_{H'}^2 - 2\lambda^x \left(v_\varphi^2 + v_\chi^2 + v^2 + 3v_\phi^2 + v_\rho^2 + 2v_s^2\right) > 0, \tag{B25}$$

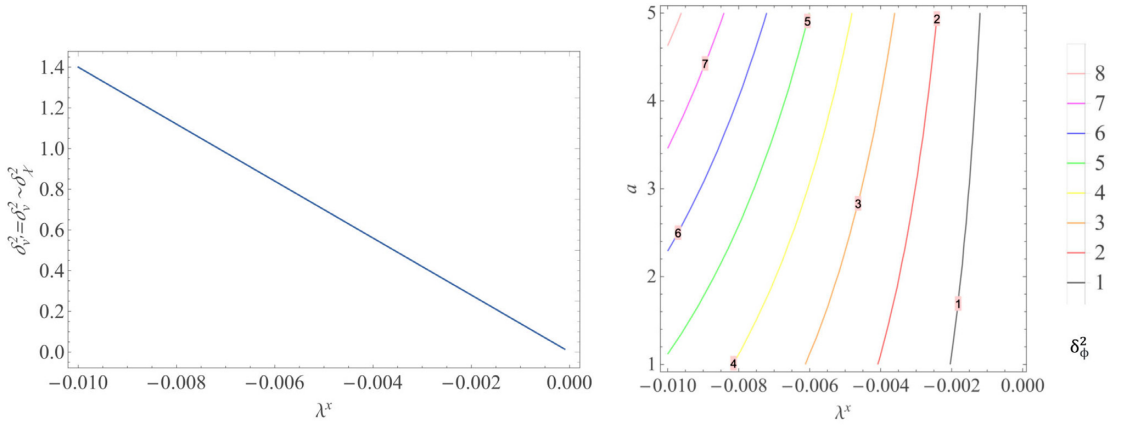

Fig. B1. $\delta_v^2 = \delta_{v'}^2 \simeq \delta_\chi^2$ versus λ^x (in the left panel), and δ_ϕ^2 versus λ^x and a (in the right panel) with $\lambda^x \in (-10^{-2}, -10^{-4})$ and $a \in (1.0, 5.0)$.

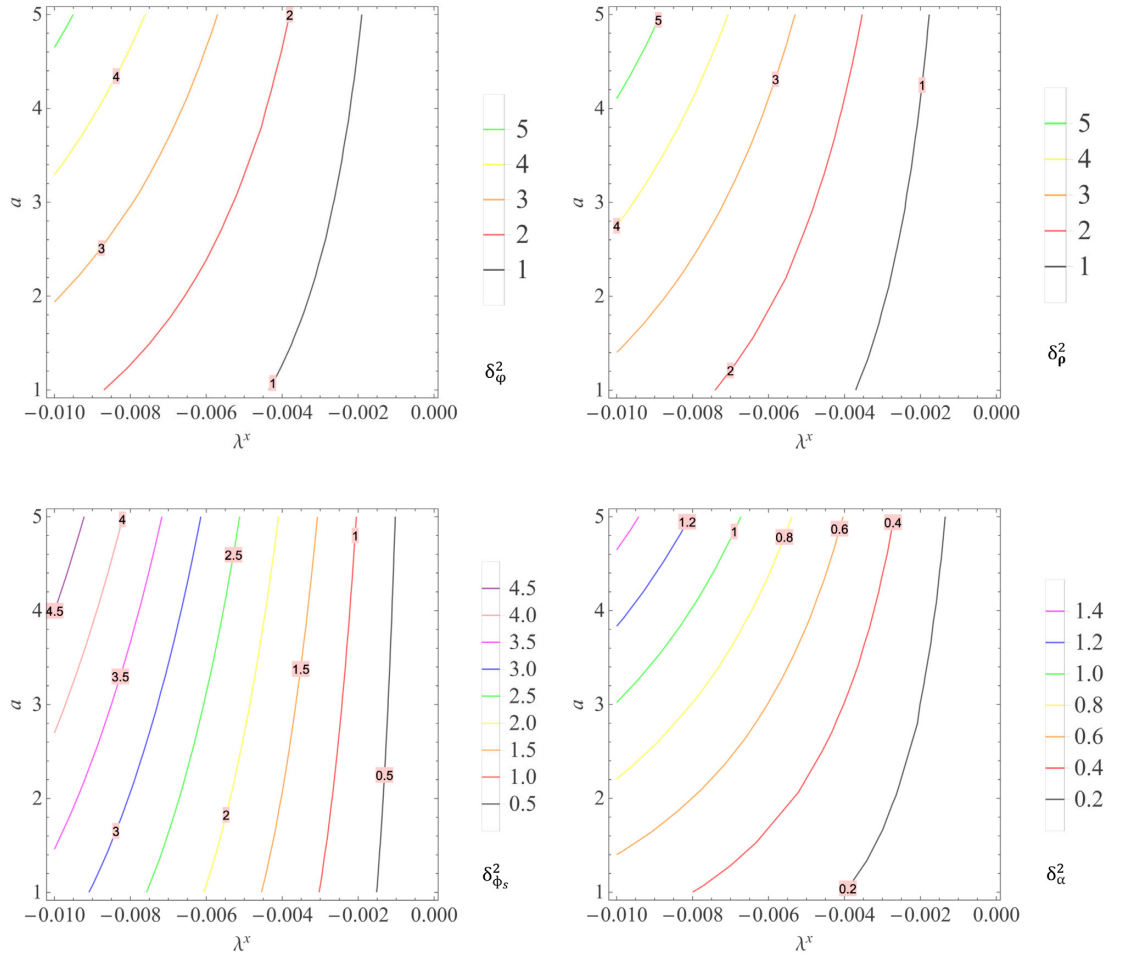

Fig. B2. δ_φ^2 (upper left), δ_ρ^2 (upper right), $\delta_{\phi_s}^2$ (bottom left), and δ_α^2 (bottom right) versus λ^x and a with $\lambda^x \in (-10^{-2}, -10^{-4})$ and $a \in (1.0, 5.0)$.

$$\delta_{\phi}^2 \sim -3\mu_{\phi}^2 - \lambda^x \Bigg[6v^2 + 6v_{\varphi}^2 + 6\left(v_{\chi}^2 + v'^2 + v_{\rho}^2\right) + 20v_s^2 + \frac{v_{\varphi} v_{\rho} \left[a v_{\phi} \left(21 a v_s + 16 v_{\phi}\right) + 3 v_s \left(9 a v_s + 7 v_{\phi}\right)\right]}{v_{\phi} \sqrt{3 a v_s + 2 v_{\phi}} \sqrt{2 a v_{\phi} + 3 v_s}} \Bigg] > 0, \tag{B26}$$

$$\delta_{\varphi}^2 \sim -\mu_{\varphi}^2 - 2\lambda^x \left(v^2 + v_{\chi}^2 + v'^2 + 3v_{\phi}^2 + v_{\rho}^2\right) - \frac{3\lambda^x v_{\phi} v_{\rho} \sqrt{\left(2 a v_{\phi} + 3 v_s\right)\left(2 v_{\phi} + 3 a v_s\right)}}{v_{\varphi}} > 0, \tag{B27}$$

$$\delta_{\rho}^2 \sim -\mu_{\rho}^2 - 2\lambda^x \left(v^2 + v_{\chi}^2 + v'^2 + 3v_{\phi}^2 + v_{\varphi}^2\right) - \frac{3\lambda^x v_{\phi} v_{\varphi} \sqrt{\left(2 a v_{\phi} + 3 v_s\right)\left(2 v_{\phi} + 3 a v_s\right)}}{v_{\rho}} > 0, \tag{B28}$$

$$\delta_{\chi}^2 = -\mu_{\chi}^2 - 2\lambda^x \left(v^2 + v_{\varphi}^2 + v'^2 + 3v_{\phi}^2 + v_{\rho}^2 + 2v_s^2\right) > 0, \tag{B29}$$

$$\delta_{\phi_s}^2 \sim -2\mu_{\phi_s}^2 - 4\lambda^x \left(v^2 + v_{\chi}^2 + v'^2 + 5v_{\phi}^2 + v_{\rho}^2\right) - \frac{9\lambda^x v_{\varphi} v_{\phi} v_{\rho} \left(v_{\phi} + a^2 v_{\phi} + 3 a v_s\right)}{v_s \sqrt{\left(2 a v_{\phi} + 3 v_s\right)\left(2 v_{\phi} + 3 a v_s\right)}} > 0,$$

$$\delta_{\alpha}^2 \sim -\lambda^x v_{\varphi} v_{\phi} v_{\rho} \sqrt{3 a v_s + 2 v_{\phi}} \sqrt{2 a v_{\phi} + 3 v_s} > 0. \tag{B30}$$

Assuming that μ_H^2, $\mu_{H'}^2$, μ_{ϕ}^2, μ_{φ}^2, μ_{ρ}^2, μ_{χ}^2, and $\mu_{\phi_s}^2$ are negative and of the same order of magnitude and also the same as that of the SM [61][5],

$$\mu_H^2 \sim \mu_{H'}^2 \sim \mu_{\phi}^2 \sim \mu_{\varphi}^2 \sim \mu_{\rho}^2 \sim \mu_{\chi}^2 \sim \mu_{\phi_s}^2 \sim -10^4\,\text{GeV}. \tag{B31}$$

Expressions (4), (5), (B25)–(B30), and (B31) tell us that $\delta_v^2 = \delta_{v'}^2$ and δ_{χ}^2 depend on one parameter λ^x while δ_{ϕ}^2, δ_{φ}^2, δ_{ρ}^2, $\delta_{\phi_s}^2$, and δ_{α}^2 depend on two parameters λ^x and a, which are respectively

[5] In the SM [61], $|\mu| = 88.4$ GeV. Here, we use $|\mu_H| \sim |\mu_{\phi}| \sim |\mu_l| \sim |\mu_v| = 10^2$ GeV for their scales.

plotted in Figs. B1 and B2 with $\lambda^x \in (-10^{-2}, -10^{-4})$ and $a \in (1.0, 5.0)$. These figures imply that the expressions (B25)–(B30) are always satisfied by the VEV alignments in Eq. (3).

Appendix C. The dependence of $|U_{ij}|$ $(i = 1, 2, 3;\ j = 1, 3)$ on s_{13} and s_{23} for normal hierarchy

Appendix D. The dependence of $|U_{ij}|$ $(i = 1, 2, 3;\ j = 1, 3)$ on s_{13} and s_{23} for inverted hierarchy

References

[1] A. A. Aguilar-Arevalo[MiniBooNE Collaboration] et al. [MiniBooNE Collaboration], Phys. Rev. Lett. **105**, 181801 (2010).
[2] A. A. Aguilar-Arevalo[MiniBooNE Collaboration] et al. [MiniBooNE Collaboration], Phys. Rev. Lett. **110**, 161801 (2013).
[3] K. Abe[Super-Kamiokande Collaboration] et al. [Super-Kamiokande Collaboration], Phys. Rev. D **91**, 052019 (2015).

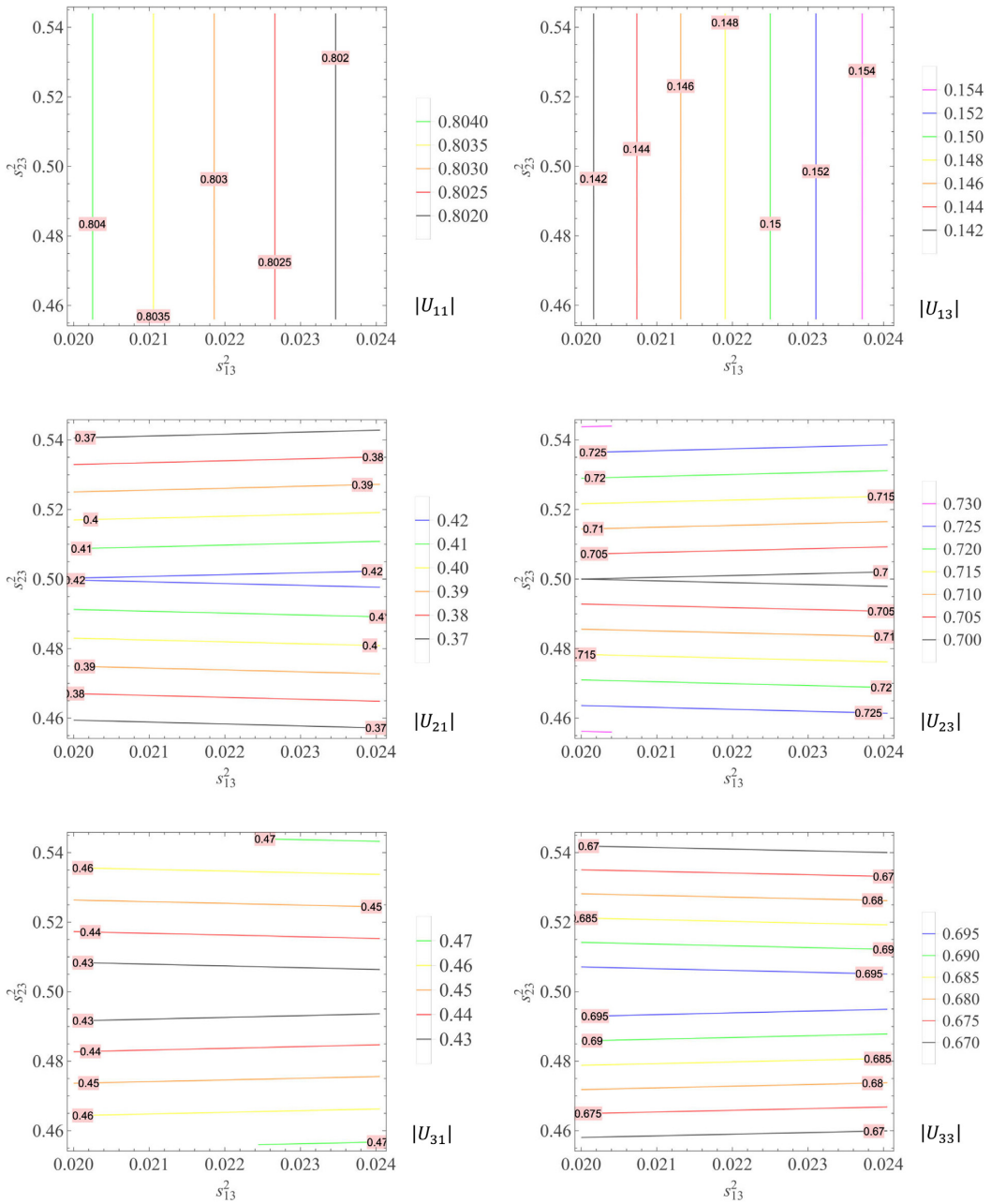

Fig. C1. $|U_{ij}|\,(i = 1, 2, 3;\ j = 1, 3)$ as functions of s^2_{23} and s^2_{13} with $s^2_{23} \in (0.456, 0.544)$ and $s^2_{13} \in (2.00, 2.405)10^{-2}$ for NH.

[4] A. A. Aguilar-Arevalo[MiniBooNE Collaboration] et al. [MiniBooNE Collaboration], Phys. Rev. Lett. **121**, 221801 (2018).
[5] S. P. Behera, D. K. Mishrab, and L. M. Pant, Eur. Phys. J. C **79**, 86 (2019).
[6] P. Adamson[Daya Bay and MINOS+ Collaborations] et al. [Daya Bay and MINOS+ Collaborations], Phys. Rev. Lett. **125**, 071801 (2020).
[7] M. G. Aartsen[IceCube Collaboration] et al. [IceCube Collaboration], Phys. Rev. Lett. **125**, 141801 (2020).
[8] P. Adamson[MINOS+ Collaboration] et al. [MINOS+ Collaboration], Phys. Rev. Lett. **122**, 091803 (2019).

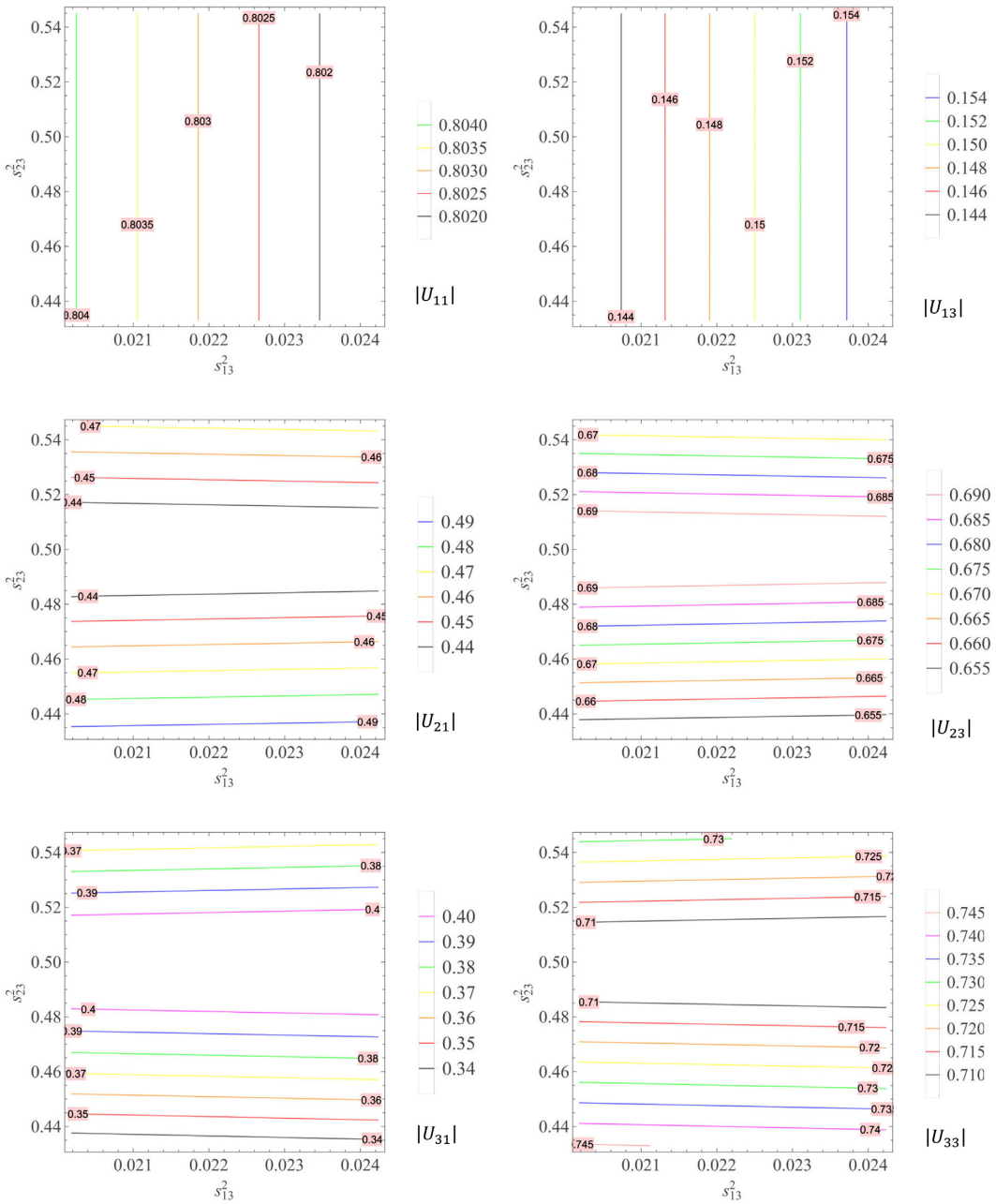

Fig. D1. $|U_{ij}|$ $(i = 1, 2, 3;\ j = 1, 3)$ as functions of s^2_{23} and s^2_{13} with $s^2_{23} \in (0.433, 0.545)$ and $s^2_{13} \in (2.018, 2.242)10^{-2}$ for IH.

[9] A. Aguilar[LSND Collaboration] et al. [LSND Collaboration], Phys. Rev. D **64**, 112007 (2001).
[10] M. A. Acero, C. Giunti, and M. Laveder, Phys. Rev. D **78**, 073009 (2008).
[11] G. Mention, M. Fechner, Th. Lasserre, Th. A. Mueller, D. Lhuillier, M. Cribier, and A. Letourneau, Phys. Rev. D **83**, 073006 (2011).
[12] F. P. An[Daya Bay Collaboration] et al. [Daya Bay Collaboration], Phys. Rev. Lett. **113**, 141802 (2014).
[13] S. P. Behera, D. K. Mishra, and L. M. Pant, Phys. Rev. D **102**, 013002 (2020).
[14] S. K. Kang, Y.-D. Kim, Y.-J. Ko, and K. Siyeon, Adv. High Energy Phys. **2013**, 138109 (2013).
[15] Ivan Girardi, Davide Melon, Tommy Ohlsson, He Zhang, and Shun Zhou, J. High Energy Phys. **1408**, 057 (2014).
[16] D. C. Rivera-Agudelo and A. Pérez-Lorenzana, Phys. Rev. D **92**, 073009 (2015).

[17] S. Gariazzo, C. Giunti, M. Laveder, and Y. F. Li, J. High Energy Phys. **2017**, 135 (2017).
[18] Valentin Hirschi, Fabio Maltoni, Ioannis Tsinikos, and Eleni Vryonidou, J. High Energy Phys. **1807**, 079 (2018).
[19] J.-H. Liu and S. Zhou, Int. J. Mod. Phys. A **33**, 1850014 (2018).
[20] S. Gariazzo, C. Giunti, M. Laveder, and Y.F. Li, Phys. Lett. B **782**, 13 (2018).
[21] Mona Dentler, Álvaro Hernández-Cabezudo, Joachim Kopp, Pedro Machado, Michele Maltoni, Ivan Martinez-Soler, and Thomas Schwetz, J. High Energy Phys. **1808**, 010 (2018).
[22] Shivani Gupta, Zachary M. Matthews, Pankaj Sharma, and Anthony G. Williams, Phys. Rev. D **98**, 035042 (2018).
[23] T. Thakore et al., J. High Energy Phys. **1808**, 022 (2018).
[24] S. Dev, Desh Raj, Radha Raman Gautam, and Lal Singh, Nucl. Phys. B **941**, 401 (2019).
[25] L. S. Miranda and S. Razzaque, J. High Energy Phys. **1903**, 203 (2019).
[26] C. Giunti and T. Lasserre, Ann. Rev. Nucl. Part. Sci. **69**, 163 (2019).
[27] Sebastian Böser, Christian Buck, Carlo Giunti, Julien Lesgourgues, Livia Ludhova, Susanne Mertens, Anne Schukraf, and Michael Wurm, Prog. Part. Nucl. Phys. **111**, 103736 (2020).
[28] C. Giunti, Y.F. Li, and Y.Y. Zhang, J. High Energy Phys. **2005**, 061 (2020).
[29] A. Diaz, C.A. Argüelles, G.H. Collin, J.M. Conrad, and M.H. Shaevitz, Phys. Rep. **884**, 1 (2020).
[30] A. E. Nelson, Phys. Rev. D **84**, 053001 (2011).
[31] J. Fan and P. Langacker, J. High Energy Phys. **1204**, 083 (2012).
[32] E. Kuflik, S. D. McDermott, and K. M. Zurek, Phys. Rev. D **86**, 033015 (2012).
[33] J. Huang and A. E. Nelson, Phys. Rev. D **88**, 033016 (2013).
[34] C. Giunti, M. Laveder, Y. F. Li, and H. W. Long, Phys. Rev. D **88**, 073008 (2013).
[35] Joachim Kopp, Michele Maltoni, and Thomas Schwetz, Phys. Rev. Lett. **107**, 091801 (2011).
[36] Joachim Kopp, Pedro A. N. Machado, Michele Maltoni, and Thomas Schwetz, J. High Energy Phys. **2013**, 50 (2013).
[37] S. Goswami and W. Rodejohann, J. High Energy Phys. **0710**, 073 (2007).
[38] M. Sorel, J. M. Conrad, and M. H. Shaevitz, Phys. Rev. D **70**, 073004 (2004).
[39] G. Karagiorgi, A. Aguilar-Arevalo, J. M. Conrad, M. H Shaevitz, K. Whisnant, M. Sorel, V. Barger, et al., Phys. Rev. D **75**, 013011 (2007).
[40] M. Maltoni and T. Schwetz, Phys. Rev. D **76**, 093005 (2007).
[41] G. Karagiorgi, Z. Djurcic, J. M. Conrad, M. H. Shaevitz, and M. Sorel, Phys. Rev. D **80**, 073001 (2009); **81**, 039902 (2010) [erratum].
[42] C. Giunti and M. Laveder, Phys. Rev. D **84**, 073008 (2011).
[43] A. Donini, P. Hernández, J. López-Pavón, M. Maltoni, and T. Schwetz, J. High Energy Phys. 161 (2012).
[44] Maria Archidiacono, Nicolao Fornengo, Carlo Giunti, and Alessandro Melchiorri, Phys. Rev. D **86**, 065028 (2012).
[45] P. F. de Salas, D. V. Forero, S. Gariazzo, P. Martínez-Miravé, O. Mena, C.A. Ternes, M. Tórtola, and J. W. F. Valle, J. High Energy Phys. **2102**, 071 (2021).
[46] K. N. Deepthi, S. Goswami, K. N. Vishnudath, and T. K. Poddar, Phys. Rev. D **102**, 015020 (2020).
[47] Ivan Esteban, M.C. Gonzalez-Garcia, Michele Maltoni, Thomas Schwetz, and Albert Zhou, J. High Energy Phys. **2009**, 178 (2020).
[48] A. C. B. Machado and V. Pleitez, J. Phys. G: Nucl. Part. Phys. **40**, 035002 (2013).
[49] V. V. Vien, Eur. Phys. J. C **81**, 416 (2021).
[50] J. Barry, W. Rodejohann, and H. Zhang, J. High Energy Phys. **1107**, 091 (2011).
[51] J. Barry, W. Rodejohann, and H. Zhang, J. Cosmol. Astropart. Phys. **1201**, 052 (2012).
[52] H. Zhang, Phys. Lett. B **714**, 262 (2012).
[53] D. Borah, Phys. Rev. D **95**, 035016 (2017).
[54] P. Das, A. Mukherjee, and M. K. Das, Nucl. Phys. B **941**, 755 (2019).
[55] N. Sarma, K. Bora, and D. Borah, Eur. Phys. J. C **79**, 129 (2019).
[56] R. Krishnan, A. Mukherjee, and S. Goswami, J. High Energy Phys. **2009**, 050 (2020).
[57] V. V. Vien, J. Phys. G: Nucl. Part. Phys. **49**, 085001 (2022).
[58] S. Khalil, J. Phys. G: Nucl. Part. Phys. **35**, 055001 (2008).
[59] M. Abbas and S. Khalil, J. High Energy Phys. **0804**, 056 (2008).
[60] H. Ishimori, Prog. Theor. Phys. Suppl. **183**, 1 (2010).

[61] P. A. Zyla[Particle Data Group] et al. [Particle Data Group], Prog. Theor. Exp. Phys. **2020**, 083C01 (2020).
[62] Kevin J. Kelly, Pedro A. N. Machado, Stephen J. Parke, Yuber F. Perez-Gonzalez, and Renata Zukanovich Funchal, Phys. Rev. D **103**, 013004 (2021).
[63] C. Jarlskog, Phys. Rev. Lett. **55**, 1039 (1985).
[64] D.-D. Wu, Phys. Rev. D **33**, 860 (1986).
[65] O. W. Greenberg, Phys. Rev. D **32**, 1841 (1985).
[66] M. Mitra, G. Senjanovic, and F. Vissani, Nucl. Phys. B **856**, 26 (2012).
[67] W. Rodejohann, J. Phys. G: Nucl. Part. Phys. **39**, 124008 (2012).
[68] J. D. Vergados, H. Ejiri, and F. Simkovic, Rep. Prog. Phys. **75**, 106301 (2012).
[69] M. Agostini[GERDA Collaboration] et al. [GERDA Collaboration], Phys. Rev. Lett. **120**, 132503 (2018).
[70] C. E. Aalseth[MAJORANA Collaboration] et al. [MAJORANA Collaboration], Phys. Rev. Lett. **120**, 132502 (2018).
[71] C. Alduino[CUORE Collaboration] et al. [CUORE Collaboration], Phys. Rev. Lett. **120**, 132501 (2018).
[72] A. Gando[KamLAND-Zen Collaboration] et al. [KamLAND-Zen Collaboration], Phys. Rev. Lett. **117**, 082503 (2016).
[73] M. Agostini[GERDA Collaboration] et al. [GERDA Collaboration], Science **365**, 1445 (2019).
[74] D. Adams[CUORE Collaboration] et al. [CUORE Collaboration], Phys. Rev. Lett. **124**, 122501 (2020).
[75] E. Armengaud[CUPID-Mo Collaboration] et al. [CUPID-Mo Collaboration], Phys. Rev. Lett. **126**, 181802 (2021).
[76] A. A. Aguilar-Arevalo[MiniBooNE Collaboration] et al. [MiniBooNE Collaboration], Phys. Rev. Lett. **110**, 161801 (2013).
[77] A. A. Aguilar-Arevalo[MiniBooNE Collaboration] et al. [MiniBooNE Collaboration], Phys. Rev. Lett. **105**, 181801 (2010).
[78] A. A. Aguilar-Arevalo[MiniBooNE Collaboration] et al. [MiniBooNE Collaboration], Phys. Rev. Lett. **121**, 221801 (2018).
[79] S. P. Behera, D. K. Mishrab, and L. M. Pant, Eur. Phys. J. C **79**, 86 (2019).
[80] S. P. Behera, D. K. Mishra, and L. M. Pant, Phys. Rev. D **102**, 013002 (2020).
[81] S. Gariazzo, C. Giunti, M. Laveder, and Y. F. Li, J. High Energy Phys. **1706**, 135 (2017).
[82] K. Hagiwara, R. Liao, A. D. Martin, D. Nomura, and T. Teubner, J. Phys. G: Nucl. Part. Phys. **38**, 085003 (2011).
[83] M. Davier, A. Hoecker, B. Malaescu, and Z. Zhang, Eur. Phys. J. C **77**, 827 (2017).
[84] T. Nomura and H. Okada, Phys. Dark Univ. **26**, 100359 (2019).
[85] T. Nomura and H. Okada, Phys. Rev. D **97**, 095023 (2018).
[86] T. Blum[RBC and UKQCD Collaborations] et al. [RBC and UKQCD Collaborations], Phys. Rev. Lett. **121**, 022003 (2018).
[87] A. Keshavarzi, D. Nomura, and T. Teubner, Phys. Rev. D **97**, 114025 (2018).
[88] T. Aoyama et al., Phys. Rep. **887**, 1 (2020).
[89] B. Abi et al., Phys. Rev. Lett. **126**, 141801 (2021).
[90] R. A. Diaz, R. Martinez, and J. A. Rodriguez, Phys. Rev. D **67**, 075011 (2003).
[91] F. Jegerlehner and A. Nyffeler, Phys. Rep. **477**, 1 (2009).
[92] C. Kelso, H. N. Long, R. Martinez, and F. S. Queiroz, Phys. Rev. D **90**, 113011 (2014).
[93] M. Lindner, M. Platscher, and F. S. Queiroz, Phys. Rep. **731**, 1 (2018).
[94] K. Kowalska and E. M. Sessolo, J. High Energy Phys. **2017**, 112 (2017).
[95] J. Cao, Chin. Phys. C **44**, 031001 (2020).
[96] M. Aker[KATRIN Collaboration] et al. [KATRIN Collaboration], Phys. Rev. Lett. **123**, 221802 (2019).